Supporting Information

Dearomative *gem*-diprenylation of hydroxynaphthalenes by an engineered fungal prenyltransferase

Yuanyuan Xu,[a,c,†] Dan Li,[a,c,†] Wenxuan Wang,[a,c] Kangping Xu,[a,c] Guishan Tan,[a,b] Jing Li,[b] Shu-Ming Li[d] and Xia Yu[*a,c]

[a.] *Xiangya School of Pharmaceutical Sciences, Central South University, Changsha, Hunan 410013, People's Republic of China*;

[b.] *Xiangya Hospital of Central South University, Central South University, Changsha, Hunan 410008, People's Republic of China*;

[c.] *Hunan Key Laboratory of Diagnostic and Therapeutic Drug Research for Chronic Diseases, Central South University, Changsha 410013, P. R. China*;

[d.] *Institut für Pharmazeutische Biologie und Biotechnologie, Fachbereich Pharmazie, Philipps-Universität Marburg, Robert-Koch Straße 4, 35037 Marburg, Germany*;

[*]Corresponding author: Xia Yu

E-mail address: xyu226@csu.edu.cn

[†] These authors contributed equally to this work

Table of Contents

Tables

Table S1: HR-ESI-MS data of new compounds.

Compound	Chemical formula	HR-ESI-MS data		Deviation (ppm)
		Calculated	Measured	
1D1	$C_{20}H_{24}O$	$[M+H]^+$ 281.1900	281.1900	0.0
2D1	$C_{15}H_{16}O_2$	$[M+H]^+$ 229.1223	229.1225	0.9
2D2	$C_{20}H_{24}O_2$	$[M+H]^+$ 297.1849	297.1855	2.0
3D2	$C_{20}H_{24}O_2$	$[M+H]^+$ 297.1849	297.1848	-0.3
4D1	$C_{15}H_{17}NO$	$[M+H]^+$ 228.1383	228.1385	0.9
4D2	$C_{20}H_{25}NO$	$[M+H]^+$ 296.2009	296.2018	3.0
5D1	$C_{15}H_{17}NO$	$[M+H]^+$ 228.1383	228.1395	5.3
5D2	$C_{20}H_{25}NO$	$[M+H]^+$ 296.2009	296.2015	2.0

Table S2: NMR data of prenylated compounds isolated in this study.

Compd.	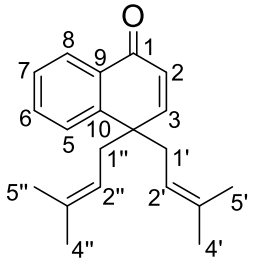 **1D1**		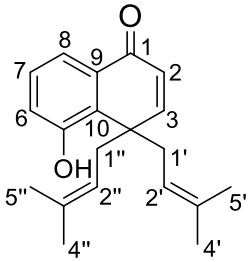 **2D2**	
Position	δ_C	δ_H, multi., *J*	δ_C	δ_H, multi., *J*
1	188.0	-	188.8	-
2	129.8	6.45, d, 10.2	128.7	6.40, d, 10.1
3	158.8	7.04, d, 10.2	161.6	6.97, d, 10.2
4	49.1	-	49.4	-
5	128.1	7.68, dd, 8.0 1.4	157.0	-
6	134.1	7.63, ddd, 8.1, 6.9, 1.4	121.0	7.01, dd, 7.9 1.3
7	127.3	7.41, ddd, 8.0, 6.8, 1.3	128.5	7.23, t, 7.9
8	127.9	8.05, dd, 7.9 1.3	118.7	7.60, dd, 7.8 1.3
9	135.7	-	135.7	-
10	149.3	-	134.6	-
1'/1"	41.0	2.80, dd, 14.4 7.5 2.63, dd, 14.4 7.5	36.5	3.52, dd, 14.2, 8.0 2.42, dd, 14.2 7.1
2'/2"	120.0	4.65, overlaps	121.1	4.63, overlaps
3'/3"	135.7	-	134.8	-
4'/4"	26.0	1.45, s	26.0	1.43, s
5'/5"	18.2	1.48, s	18.1	1.50, s

Table S2 (continued): NMR data of prenylated compounds isolated in this study.

Compd.	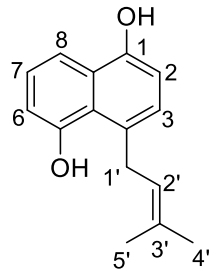 **2D1**		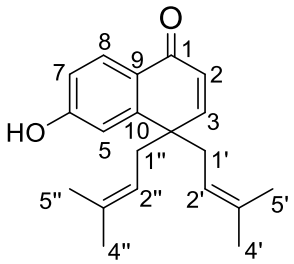 **3D2**	
Position	δ_C	δ_H, multi., *J*	δ_C	δ_H, multi., *J*
1	152.3	-	187.4	-
2	108.8	6.66, d, 7.7	129.7	6.36, d, 10.1
3	127.3	6.94, d, 7.8	157.8	6.92, d, 10.1
4	130.6	-	48.6	-
5	156.4	-	113.6	6.96, d, 2.3
6	111.1	6.77, dd, 7.5 1.3	163.6	-
7	125.5	7.15, dd, 8.4 7.5	116.0	6.81, dd, 8.7 2.3
8	114.8	7.68, dd, 8.4 1.2	129.9	7.94, d, 8.7
9	129.3	-	126.3	-
10	125.9	-	152.4	-
1'	36.1	3.96, d, 7.1	41.2	2.70, dd, 14.5 7.3 2.58, dd, 14.4 7.5
2'	127.5	5.44, m	120.0	4.65, overlaps
3'	130.8	-	135.5	-
4'	26.0	1.70, s	26.0	1.48, s
5'	18.0	1.73, s	18.2	1.51, s
1"	-	-	41.2	2.70, dd, 14.5 7.3 2.58, dd, 14.4 7.5
2"	-	-	120.0	4.65, overlaps
3"	-	-	135.5	-
4"	-	-	26.0	1.48, s
5"	-	-	18.2	1.51, s

Table S2 (continued): NMR data of prenylated compounds isolated in this study.

Compd.	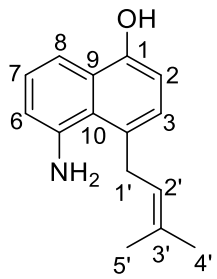 **4D1**		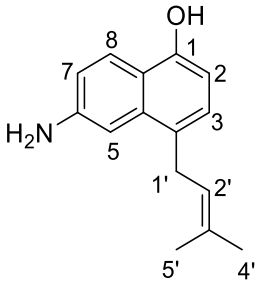 **5D1**
Position	δ_C	δ_H, multi., *J*	δ_H, multi., *J*
1	153.3	-	-
2	108.6	6.66, d, 7.7	6.45, d, 7.6
3	128.8	6.95, d, 7.7	6.95, d, 7.8
4	129.7	-	-
5	145.7	-	7.11, d, 2.2
6	114.3	6.78, dd, 7.4 1.3	-
7	125.9	7.14, dd, 8.4, 7.4	6.95, br.d, 7.8
8	114.9	7.67, dd, 8.4 1.3	7.99, d, 8.9
9	129.3	-	-
10	126.7	-	-
1'	36.9	3.87, d, 6.1	3.52, d, 7.1
2'	127.5	5.33, m	5.34, t, 7.2
3'	134.4	-	-
4'	25.9	1.77, d, 1.6	1.74, s
5'	18.4	1.79, d, 1.3	1.78, s

Table S2 (continued): NMR data of prenylated compounds isolated in this study.

Compd.	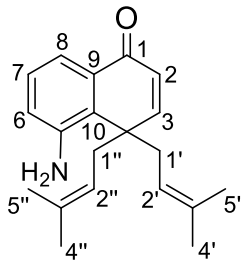 **4D2**		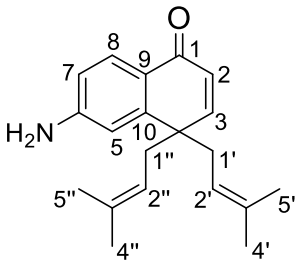 **5D2**	
Position	δ_C	δ_H, multi., *J*	δ_C	δ_H, multi., *J*
1	189.1	-	187.2	-
2	128.2	6.37, d, 10.2	129.7	6.29, d, 10.1
3	161.5	6.92, d, 10.1	156.9	6.81, d, 10.1
4	49.3	-	48.3	-
5	147.3	-	111.4	6.77, d, 2.2
6	122.9	6.95, d, 7.8	155.0	-
7	128.6	7.17, t, 7.8	114.6	6.63, d, 8.5 2.1
8	117.8	7.52, d, 7.7	129.7	7.82, d, 8.4
9	135.5	-	123.6	-
10	131.6	-	152.0	-
1'/1"	35.5	3.26, dd, 15.0 6.8 2.48, dd, 15.0 7.6	41.4	2.66, dd, 14.3 7.0 2.56, dd, 14.3 7.6
2'/2"	120.4	4.63, overlaps	120.3	4.67, m
3'/3"	135.2	-	135.1	-
4'/4"	26.0	1.45, s	26.1	1.49, s
5'/5"	18.2	1.53, s	18.3	1.53, s

Table S2 (continued): NMR data of prenylated compounds isolated in this study.

Compd.	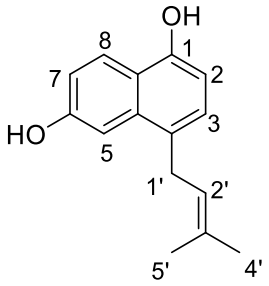 **3D1**	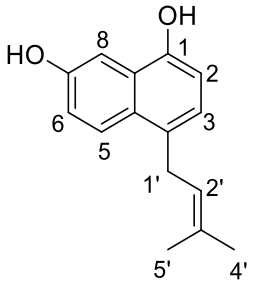 **6D1**
Position	δ_H, multi., *J*	δ_H, multi., *J*
1	-	-
2	6.51, d, 7.6	6.65, d, 7.6
3	7.00, d, 7.6	6.88, d, 7.6
4	-	-
5	7.17, d, 2.4	7.78, d, 9.1
6	-	7.05, dd, 9.1 2.6
7	6.97, m	-
8	8.07, d, 9.0	7.49, d, 2.7
9	-	-
10	-	-
1'	3.54, d, 6.4	3.59, d, 7.1
2'	5.32, m	5.31, m
3'	-	-
4'	1.75, s	1.73, s
5'	1.79, s	1.78, s

Table S3: Kinetic parameters of CdpC3PT_F253G towards **1-5**, Hs/HcPT8px and Hs/HcPTpat towards 1367THX, and AtaPT towards acylphloroglucinols in the presence of DMAPP.

substrate	donor	K_M [mM]	k_{cat} [min^{-1}]	k_{cat}/K_M [$s^{-1}M^{-1}$]
CdpC3PT_F253G				
1	DMAPP	0.64±0.11	6.53±0.37	170.6±31.3
2	DMAPP	1.14±0.14	20.28±0.98	297.8±40.3
3	DMAPP	0.41±0.04	3.17±0.09	128.3±12.8
4	DMAPP	0.61±0.10	6.59±0.34	181.6±30.3
5	DMAPP	0.76±0.10	2.11±0.09	46.1±6.3
HsPT8px[a]				
1367THX	DMAPP	0.053 ± 0.0015	9.46 ± 0.08[c] (nkat/µg micro-somal protein)	/
HsPTpat[a]				
1367THX	DMAPP	0.200 ± 0.0164	0.24 ± 0.01[c] (nkat/µg micro-somal protein)	/
AtaPT[b]				
PIBP	DMAPP	0.16 ± 0.006	17.04 ± 0.12	1775.0
PIVP	DMAPP	1.10 ± 0.035	6.18 ± 0.012	96.5
PBZP	DMAPP	0.58 ± 0.064	6.36 ± 0.30	182.8

[a] Data adopted from M. Nagia, M. Gaid, E. Biedermann, T. Fiesel, I. El-Awaad, R. Haensch, U. Wittstock and L. Beerhues, *New Phytol*, 2019, **222**, 318-334.

[b] Data adopted from K. Zhou, C. Wunsch, J. Dai and S.-M. Li, *Org Lett* 2017, **19**, 388-391.

[c] Data obtained as nkat/µg total microsomal yeast protein.

Figures

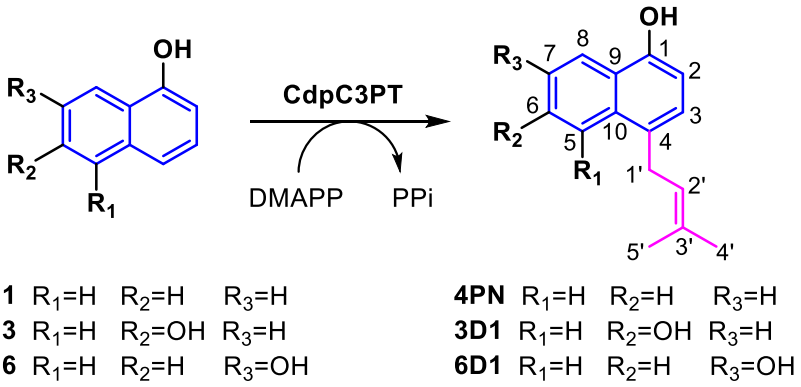

Figure S1: Products **4PN**, **3D1** and **6D1** converted in the assays catalyzed by wild-type CdpC3PT with DMAPP. (**4PN**: 4-prenylated-*α*-naphthol)

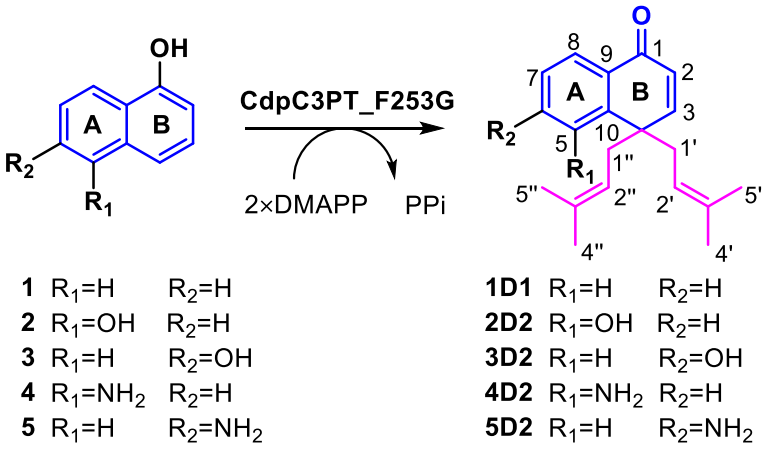

Figure S2: The dearomative *gem*-diprenylation catalyzed by CdpC3PT_F253G in this study.

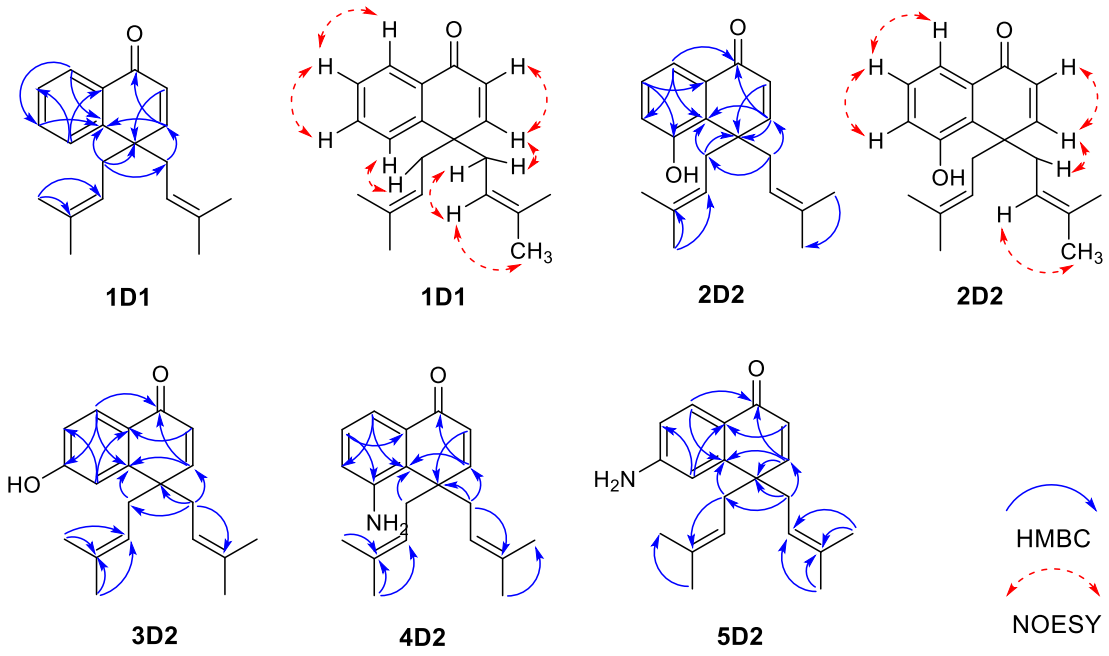

Figure S3: The key NOESY and HMBC signals of **1D1**, **2D2**, **3D2**, **4D2** and **5D2**.

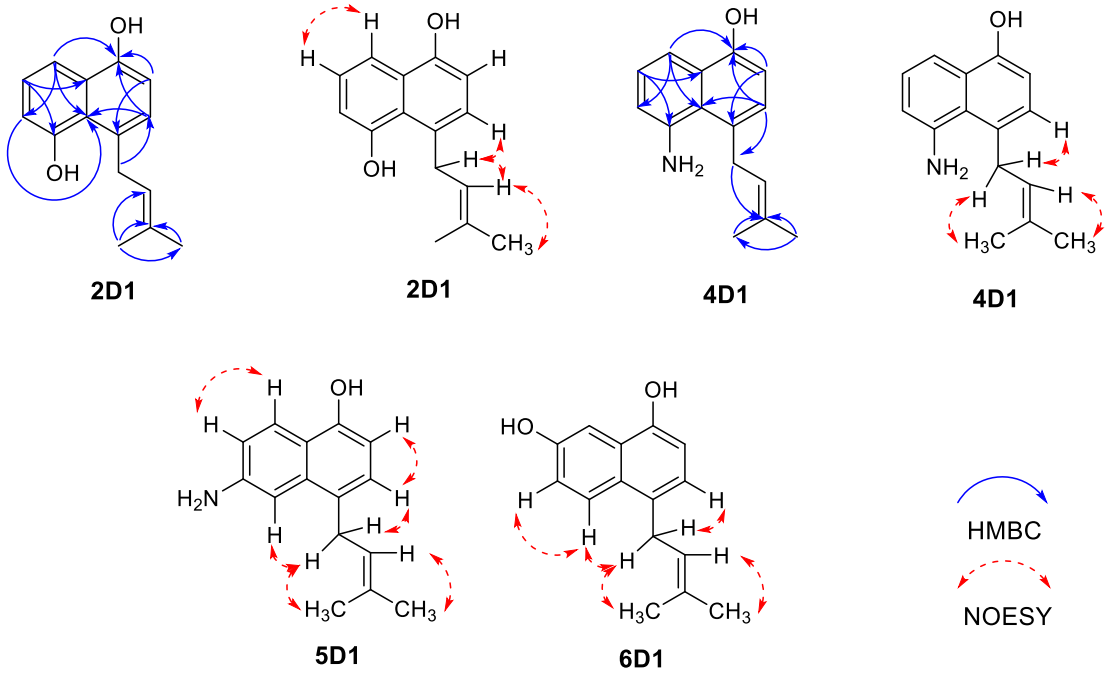

Figure S4: The key NOESY and HMBC signals of **2D1**, **4D1**, **5D1** and **6D1**.

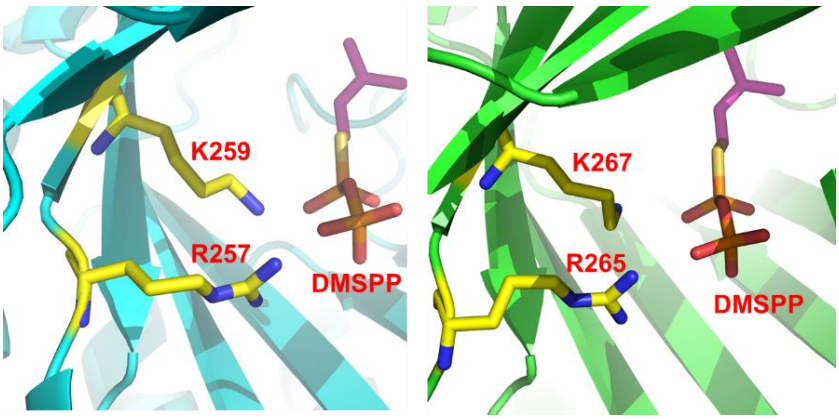

Figure S5: The conserved Lys and Arg interacting with pyrophosphate moiety in DMSPP in FgaPT2 (left) and CdpC3PT (right).

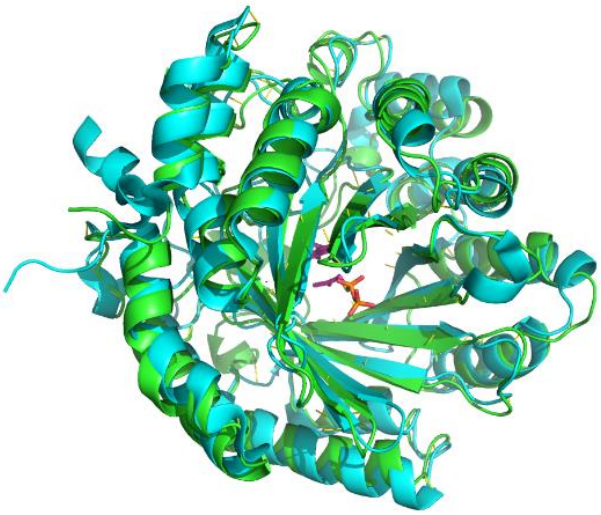

Figure S6: The aligned and overlapping docking model of FgaPT2 (PDB entry: 3I4X) and CdpC3PT, with 3I4X in blue and CdpC3PT in green.

The figure was generated by Pymol (Schrödinger, LLC.) and the RMS=1.47.

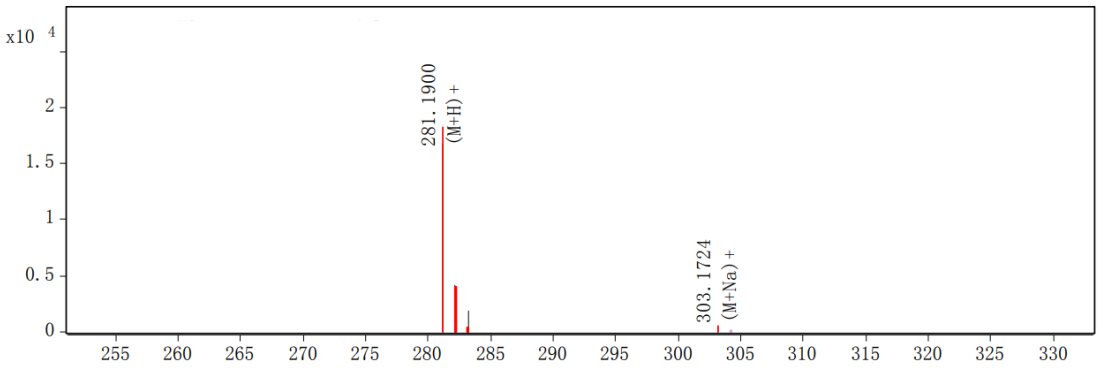

Fig S7: HR-ESI-MS spectrum of compound **1D1.**

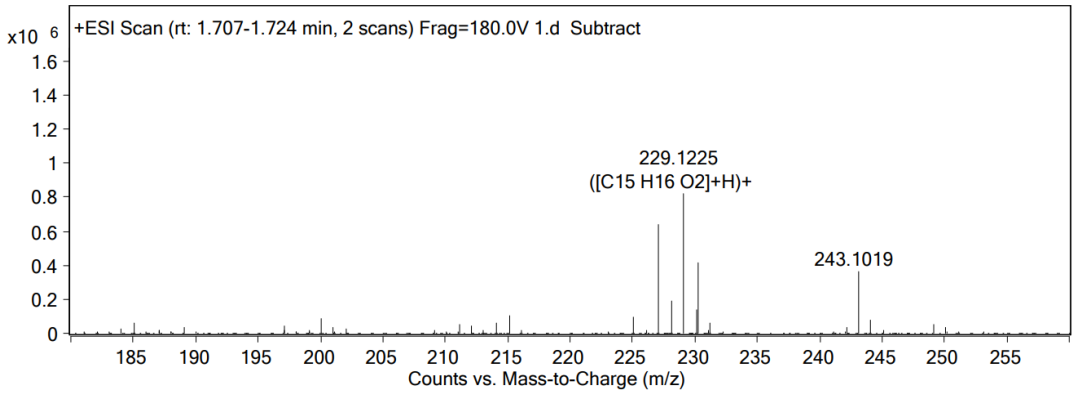

Fig S8: HR-ESI-MS spectrum of compound **2D1.**

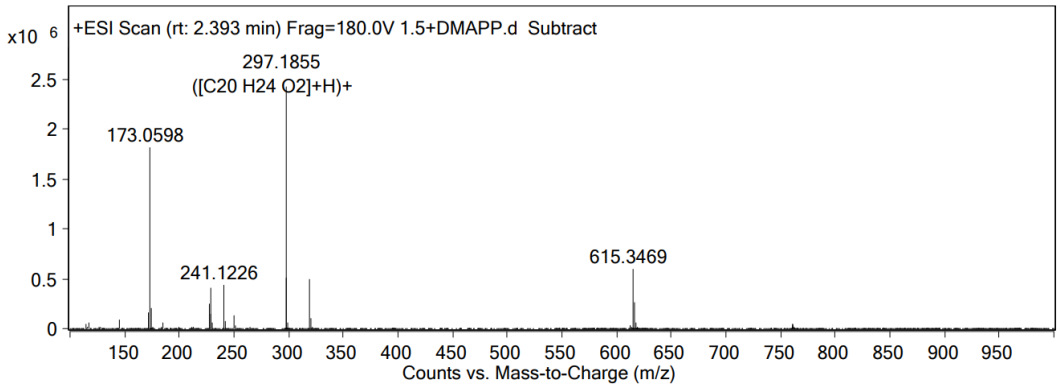

Fig S9: HR-ESI-MS spectrum of compound **2D2.**

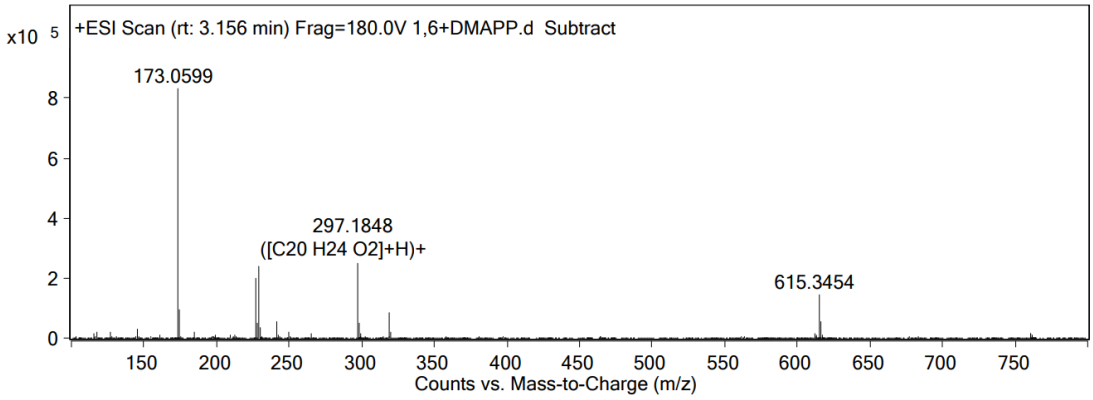

Fig S10: HR-ESI-MS spectrum of compound **3D2.**

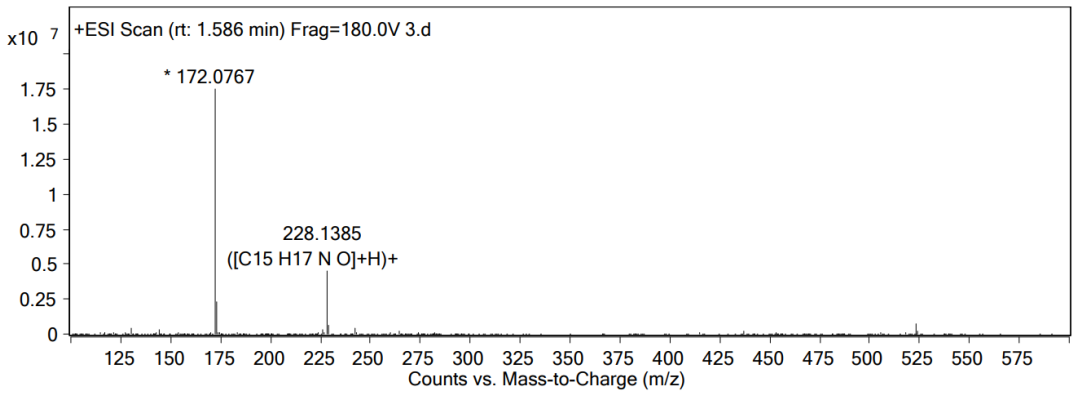

Fig S11: HR-ESI-MS spectrum of compound **4D1.**

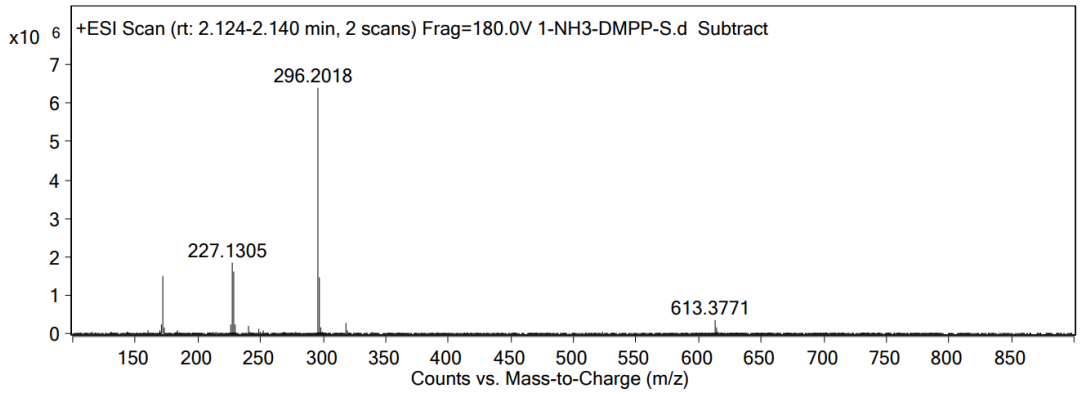

Fig S12: HR-ESI-MS spectrum of compound **4D2.**

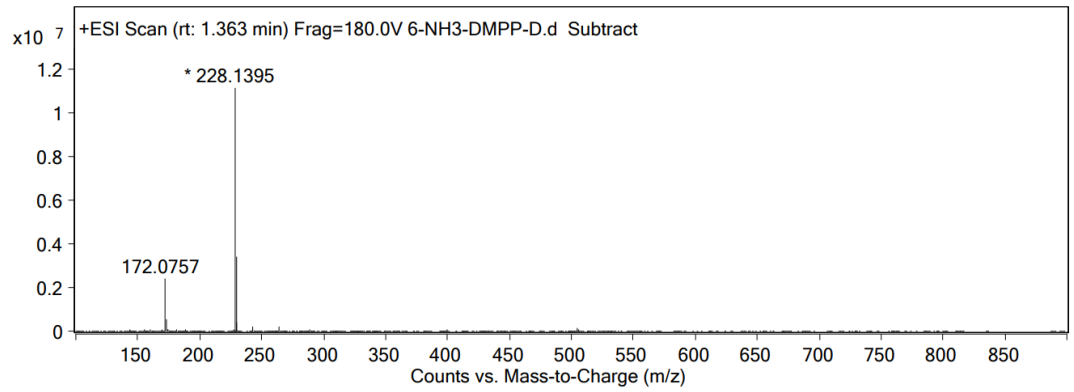

Fig S13: HR-ESI-MS spectrum of compound **5D1.**

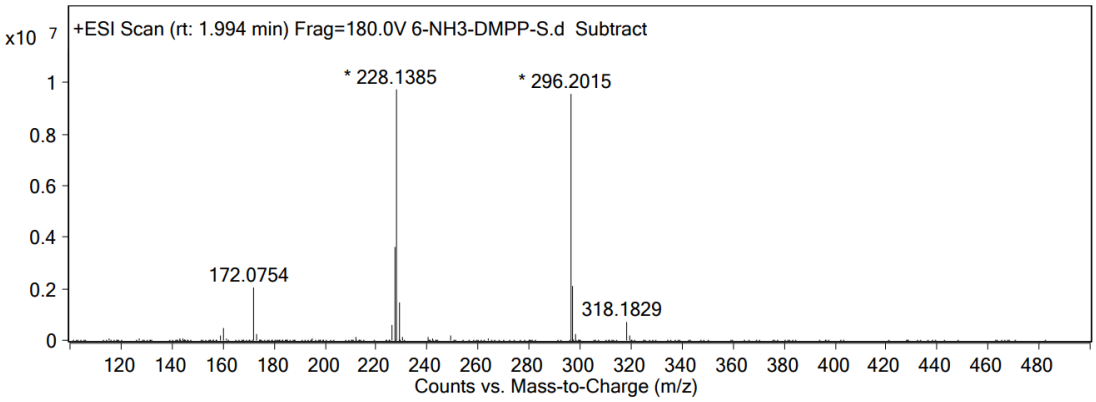

Fig S14: HR-ESI-MS spectrum of compound **5D2.**

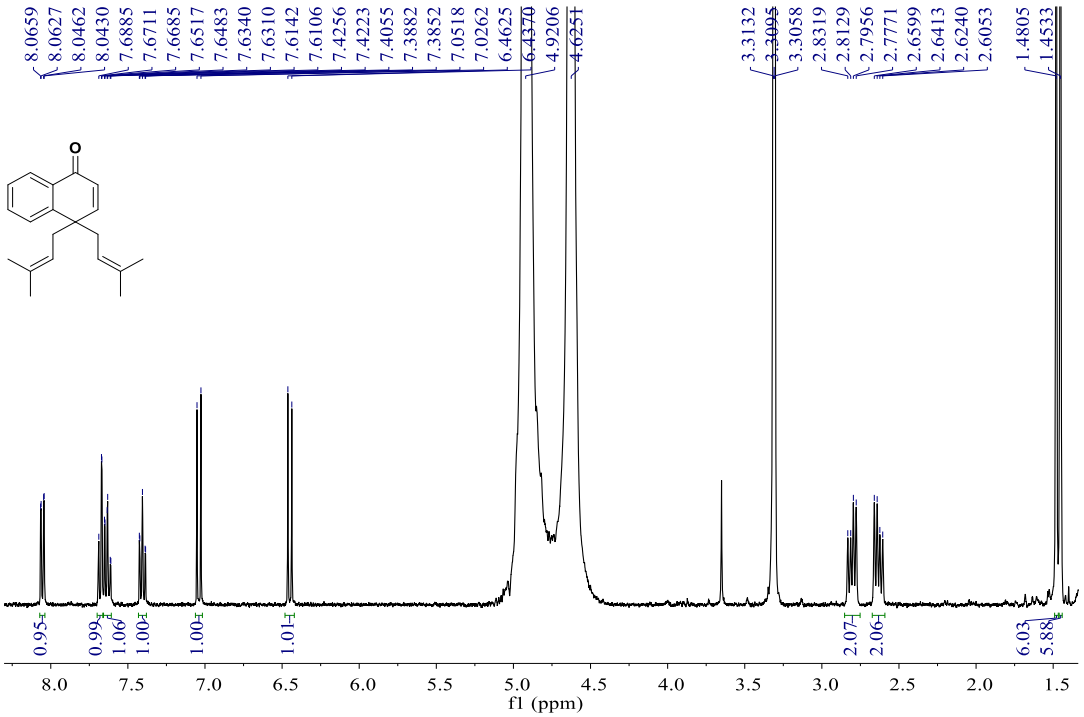

Figure S15: ^{1}H-NMR spectrum of **1D1** in CD_3OD (500 MHz).

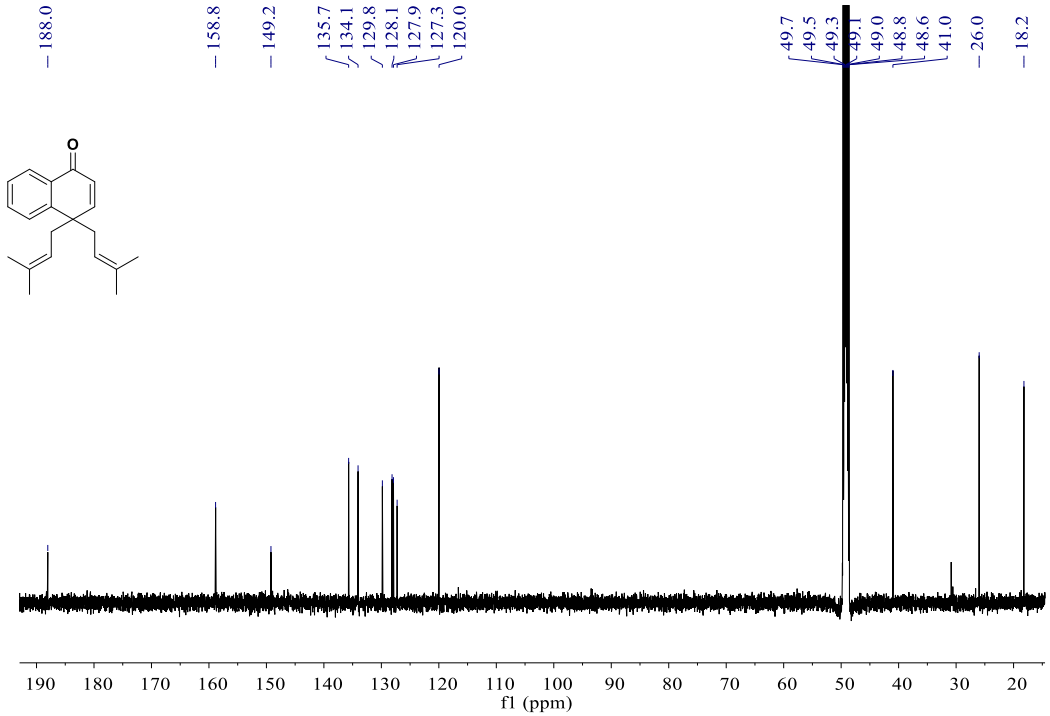

Figure S16: ^{13}C-NMR spectrum of **1D1** in CD_3OD (125 MHz).

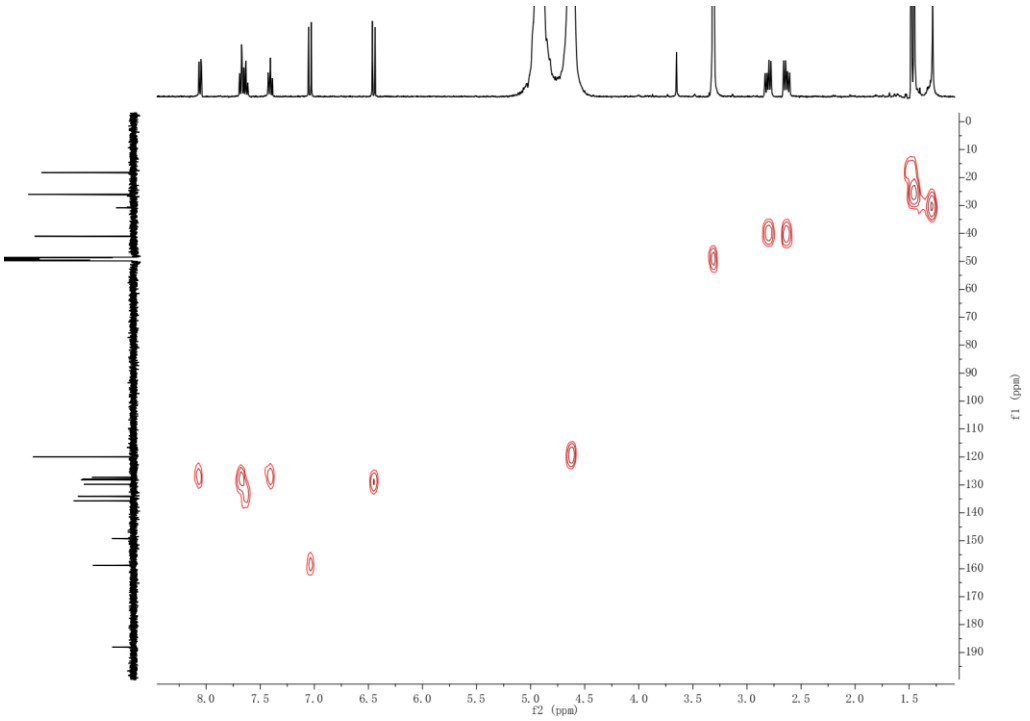

Figure S17: HSQC spectrum of **1D1** in CD_3OD (125 MHz).

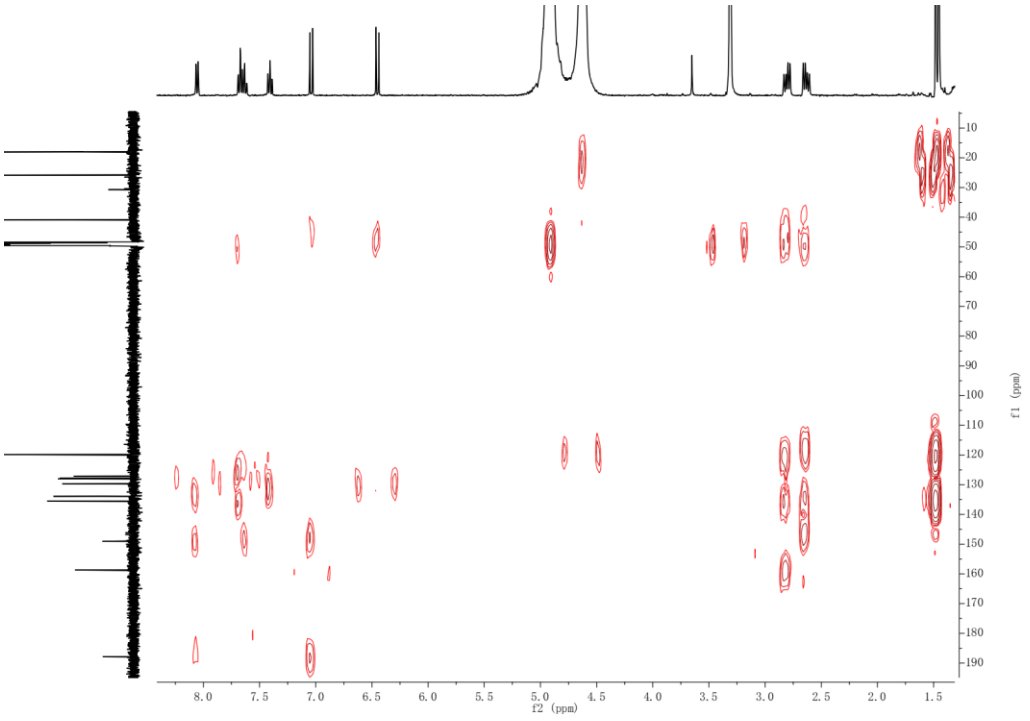

Figure S18: HMBC spectrum of **1D1** in CD_3OD (125 MHz).

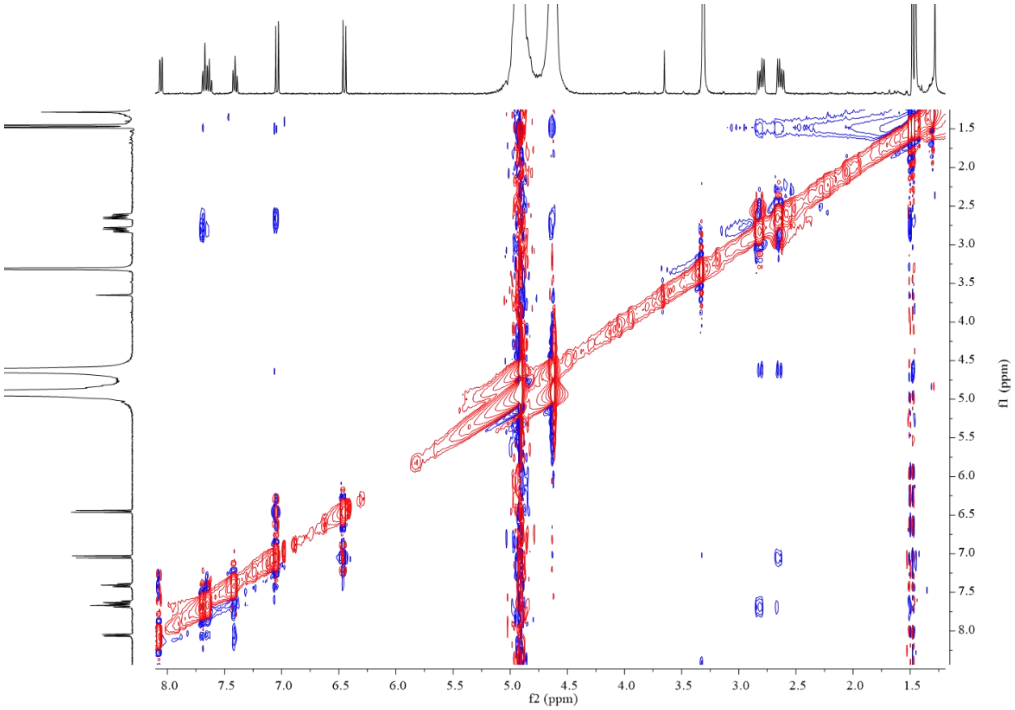

Figure S19: NOESY spectrum of **1D1** in CD_3OD (500 MHz).

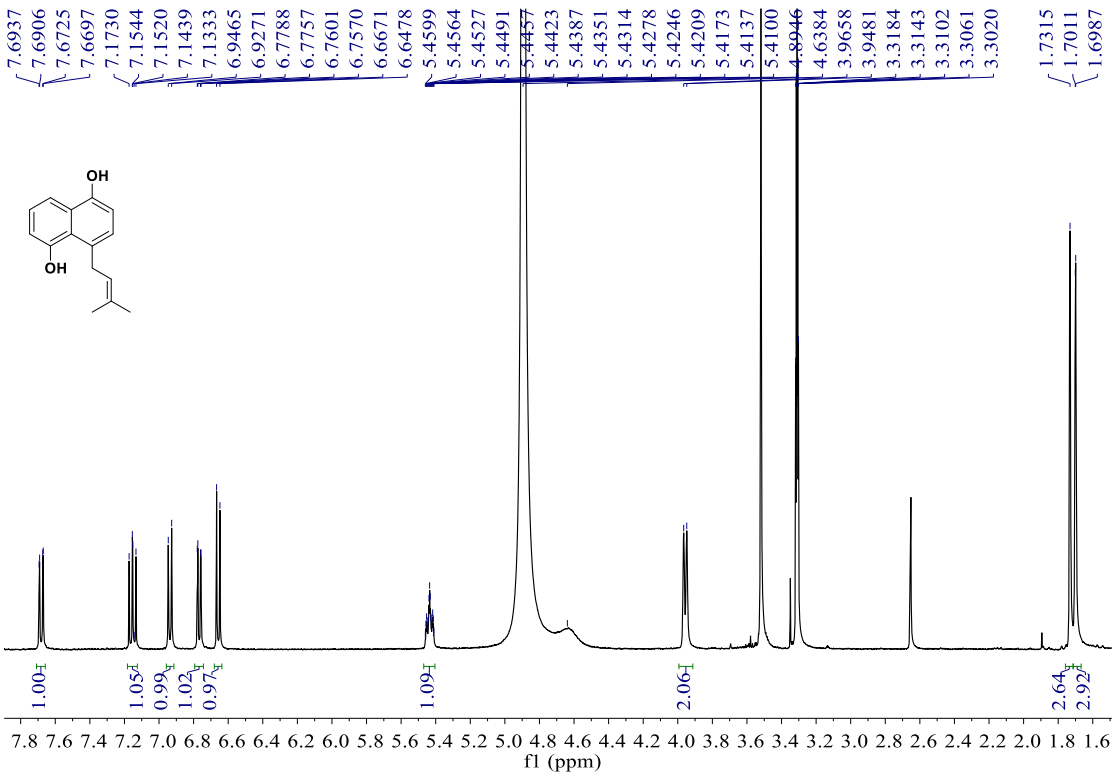

Figure S20: ^{1}H-NMR spectrum of **2D1** in CD_3OD (400 MHz).

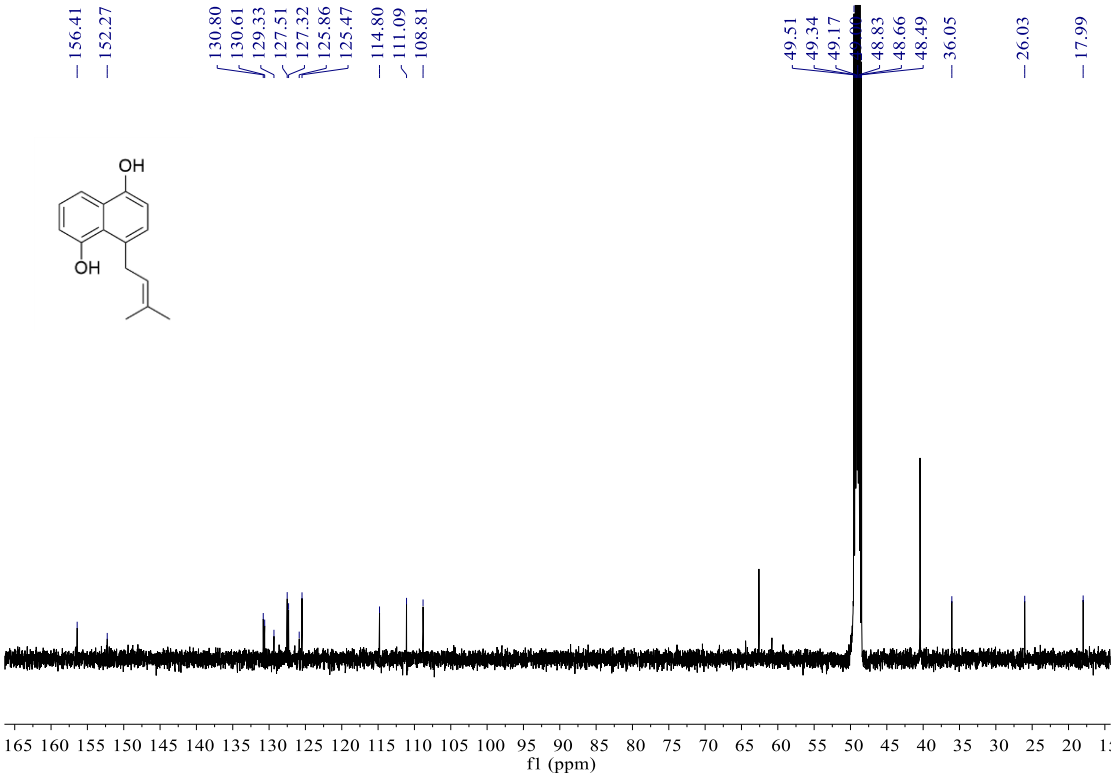

Figure S21: ^{13}C-NMR spectrum of **2D1** in CD_3OD (125 MHz).

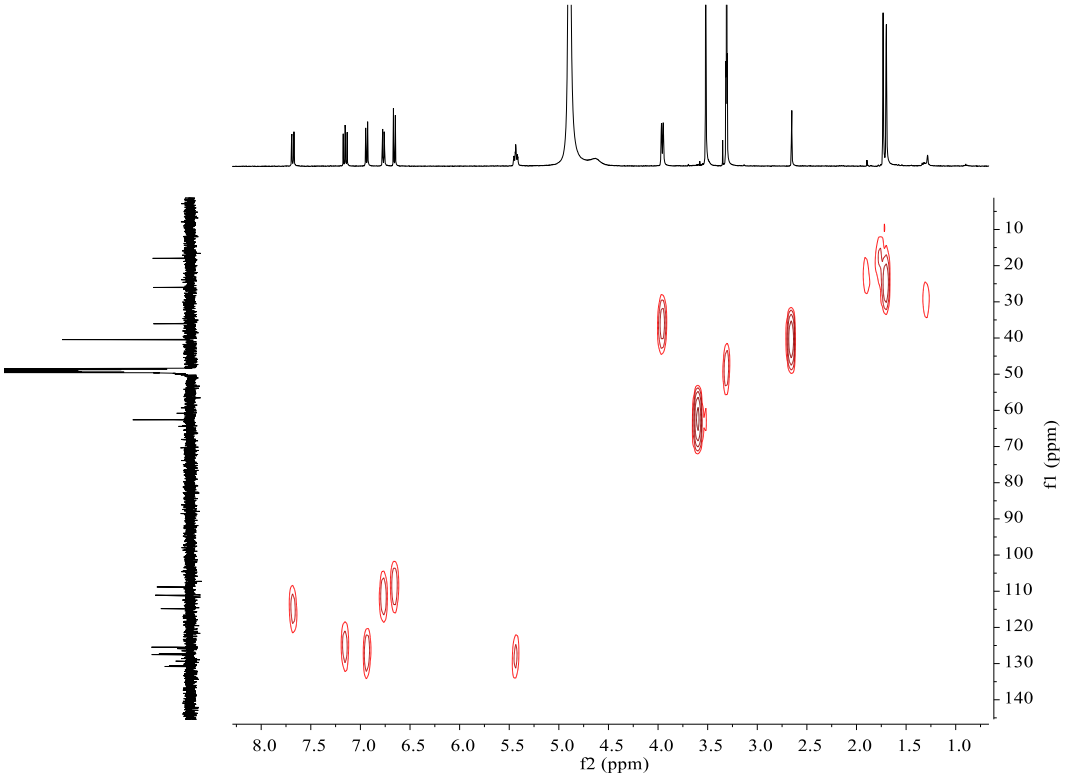

Figure S22: HSQC spectrum of **2D1** in CD_3OD (125 MHz).

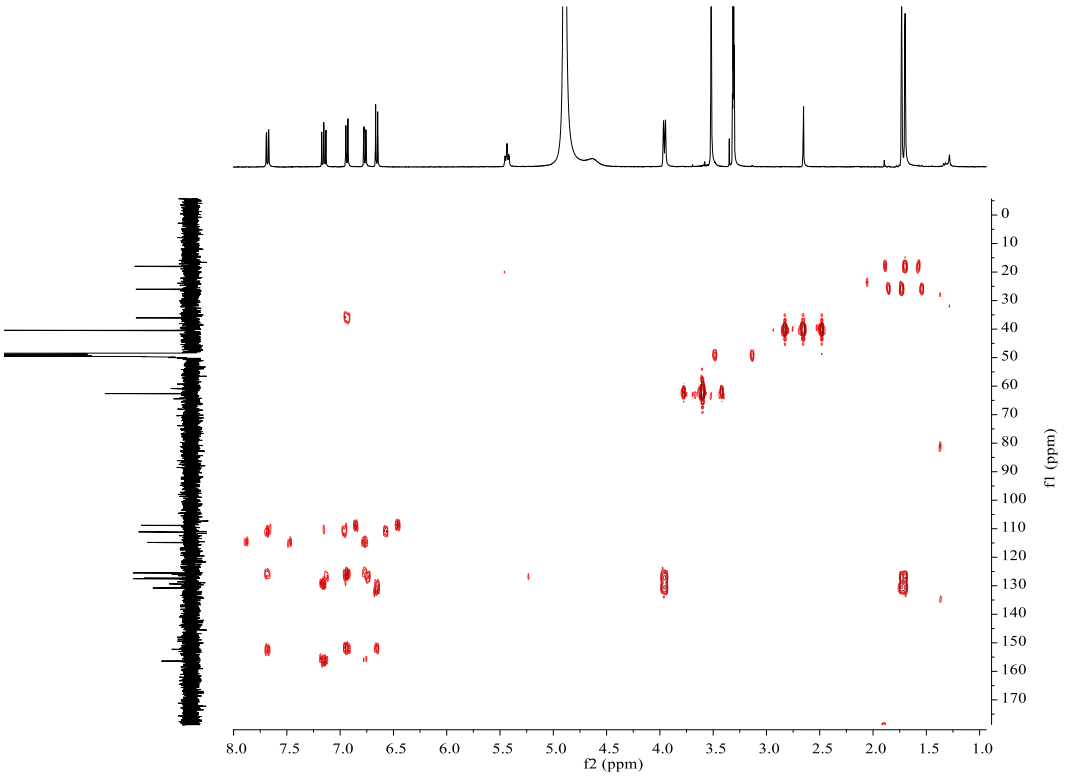

Figure S23: HMBC spectrum of **2D1** in CD_3OD (125 MHz).

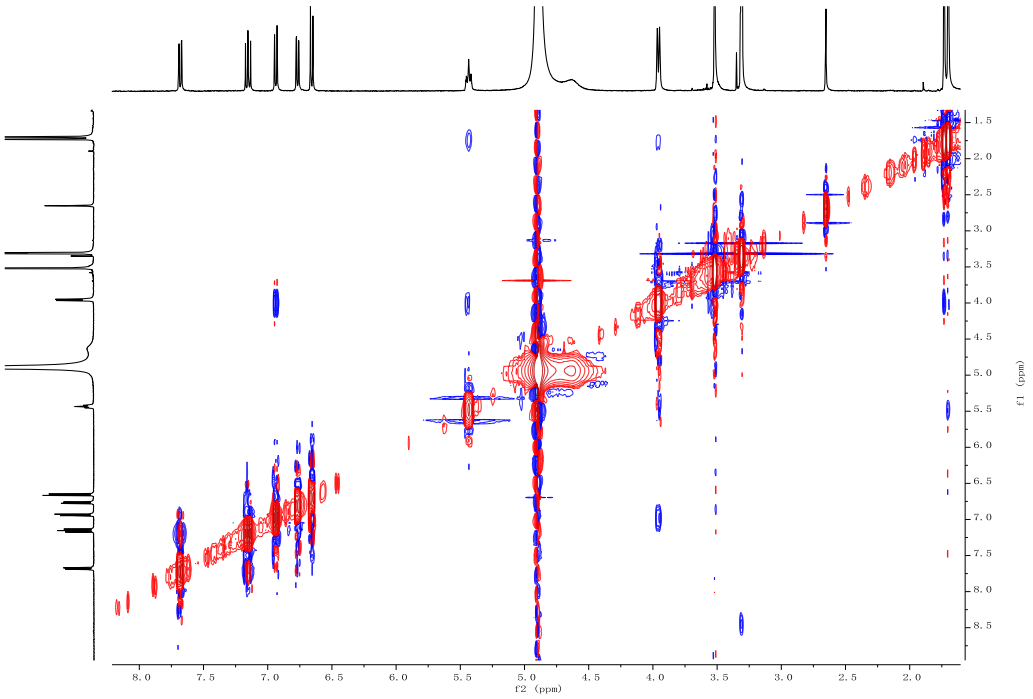

Figure S24: NOESY spectrum of **2D1** in CD_3OD (400 MHz).

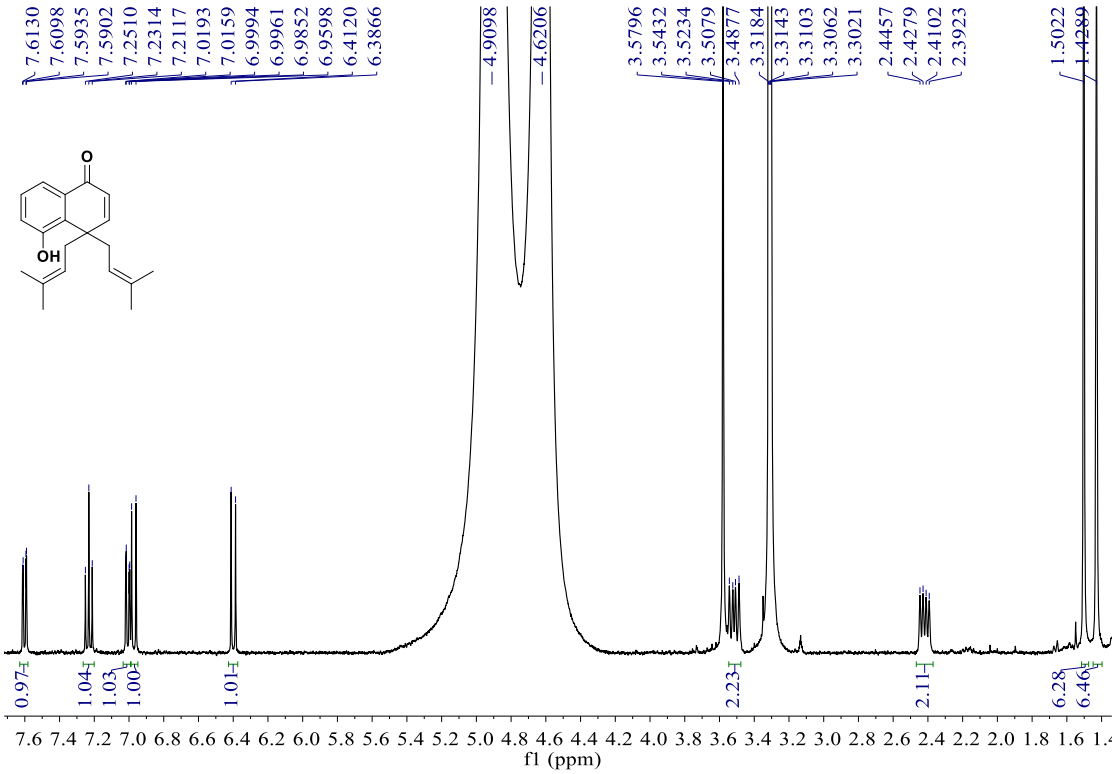

Figure S25: ^{1}H-NMR spectrum of **2D2** in CD3OD (400 MHz).

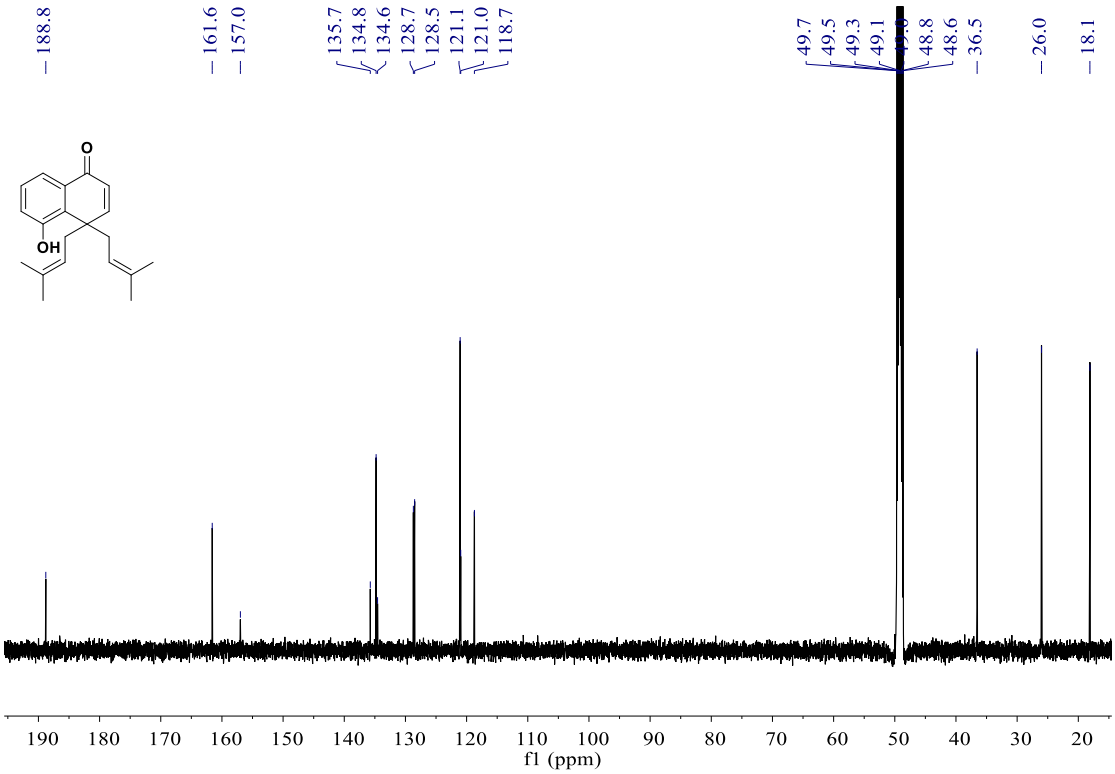

Figure S26: ^{13}C-NMR spectrum of **2D2** in CD_3OD (125 MHz).

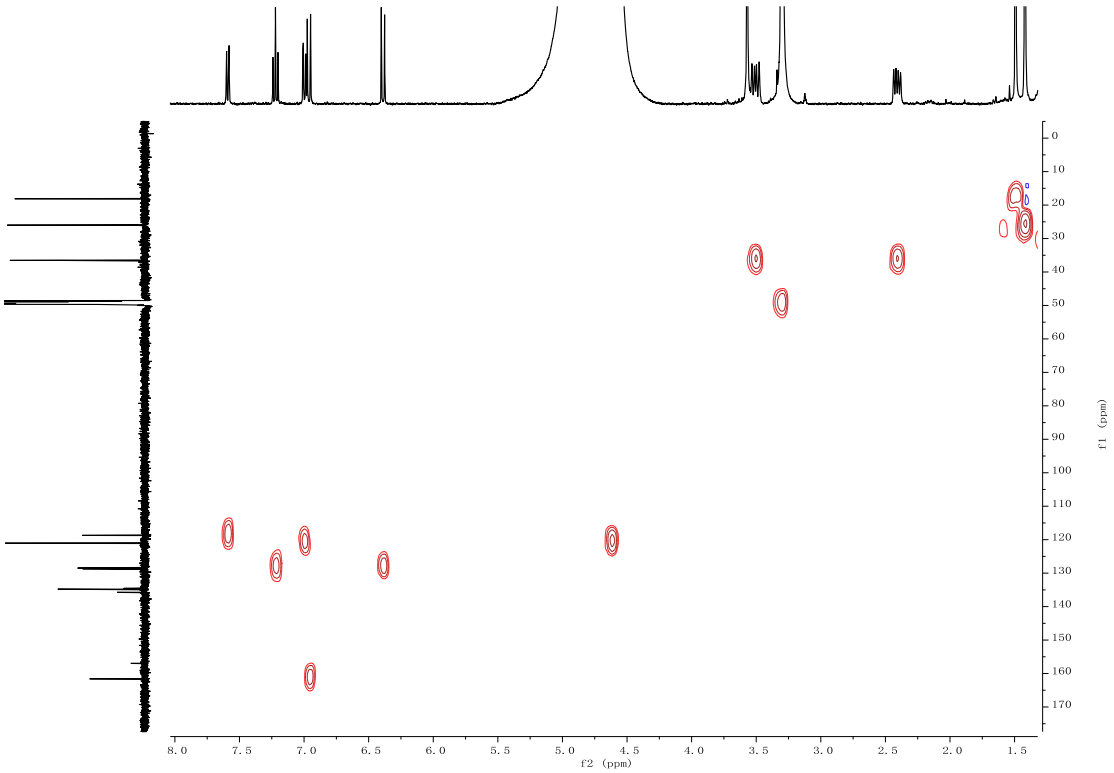

Figure S27: HSQC spectrum of **2D2** in CD_3OD (125 MHz).

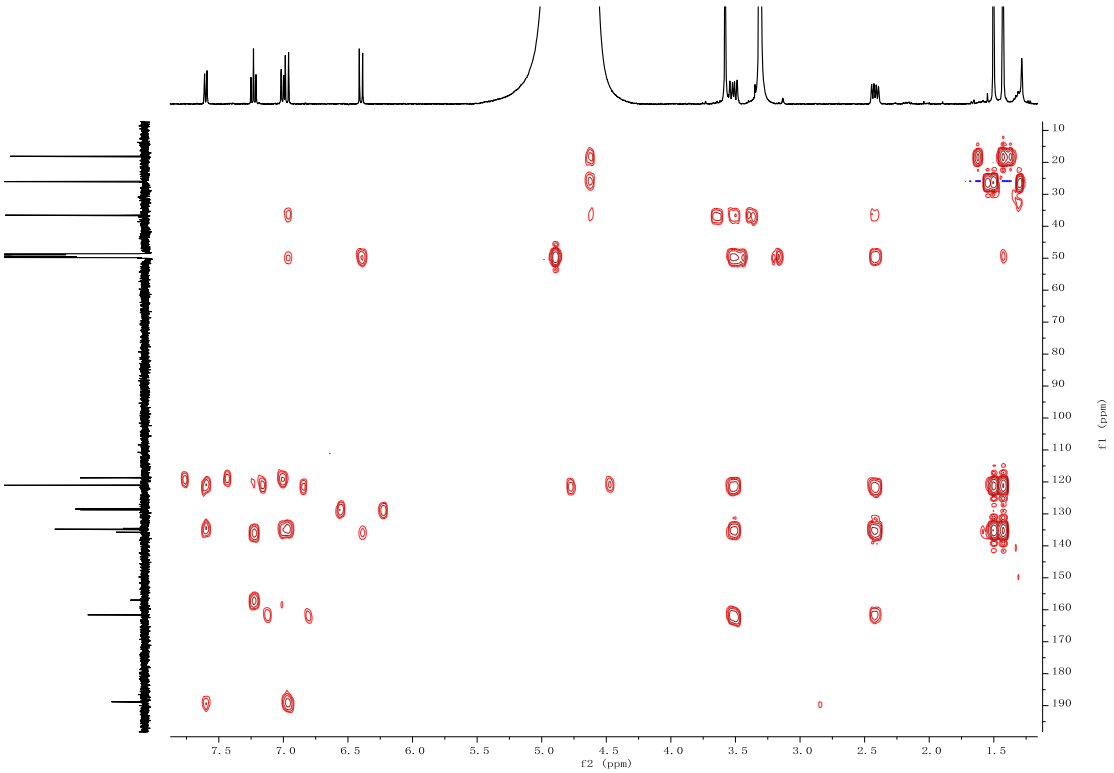

Figure S28: HMBC spectrum of **2D2** in CD_3OD **(**125 MHz).

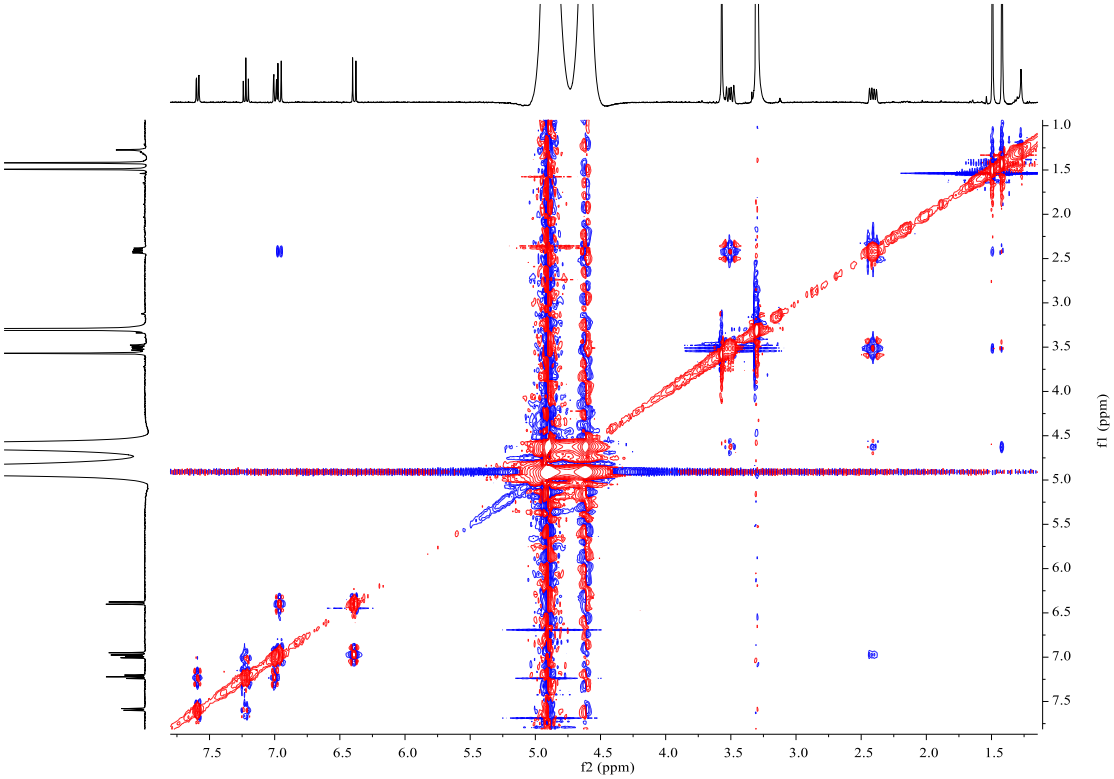

Figure S29: NOESY spectrum of **2D2** in CD_3OD (400 MHz).

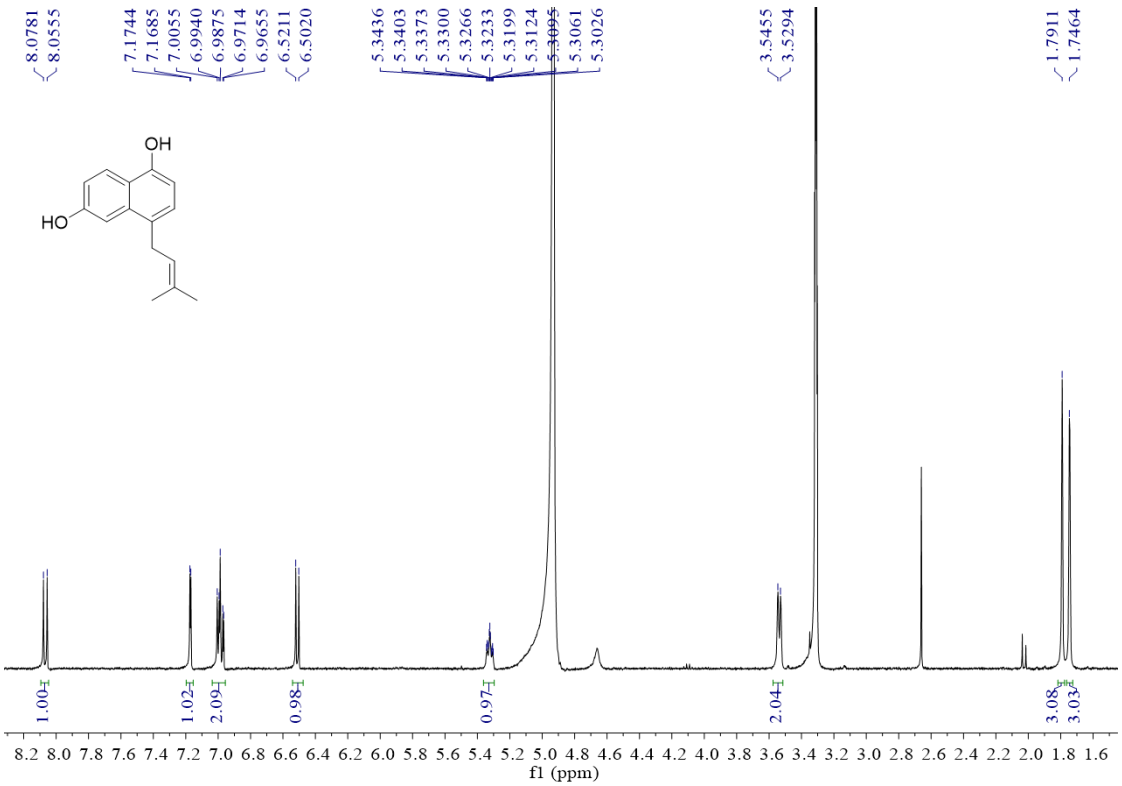

Figure S30: ^{1}H-NMR spectrum of **3D1** in CD_3OD (400 MHz).

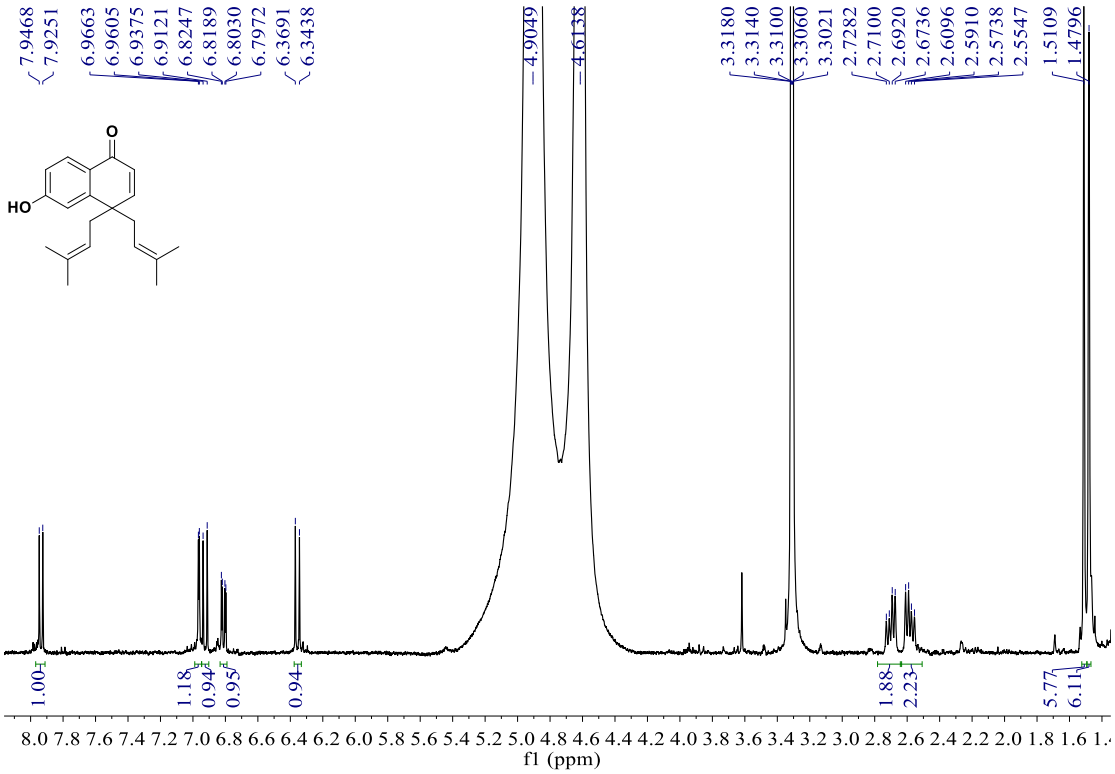

Figure S31: ^{1}H-NMR spectrum of **3D2** in CD_3OD (400 MHz).

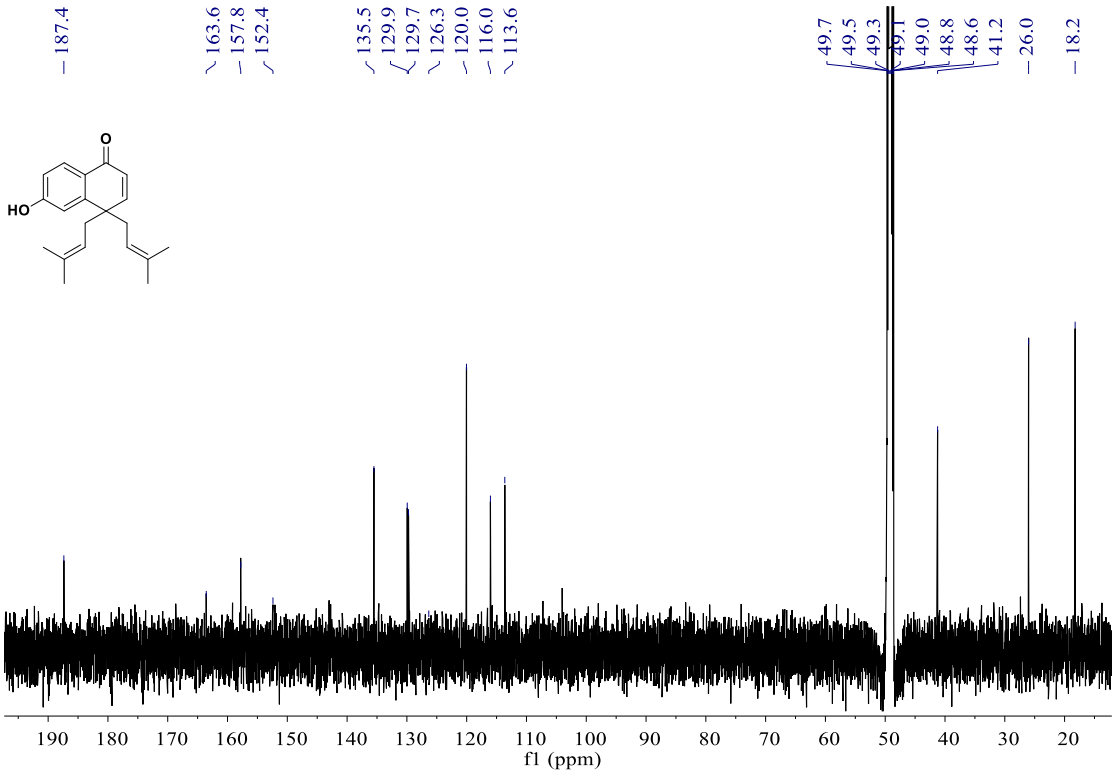

Figure S32: ^{13}C-NMR spectrum of **3D2** in CD_3OD (125 MHz).

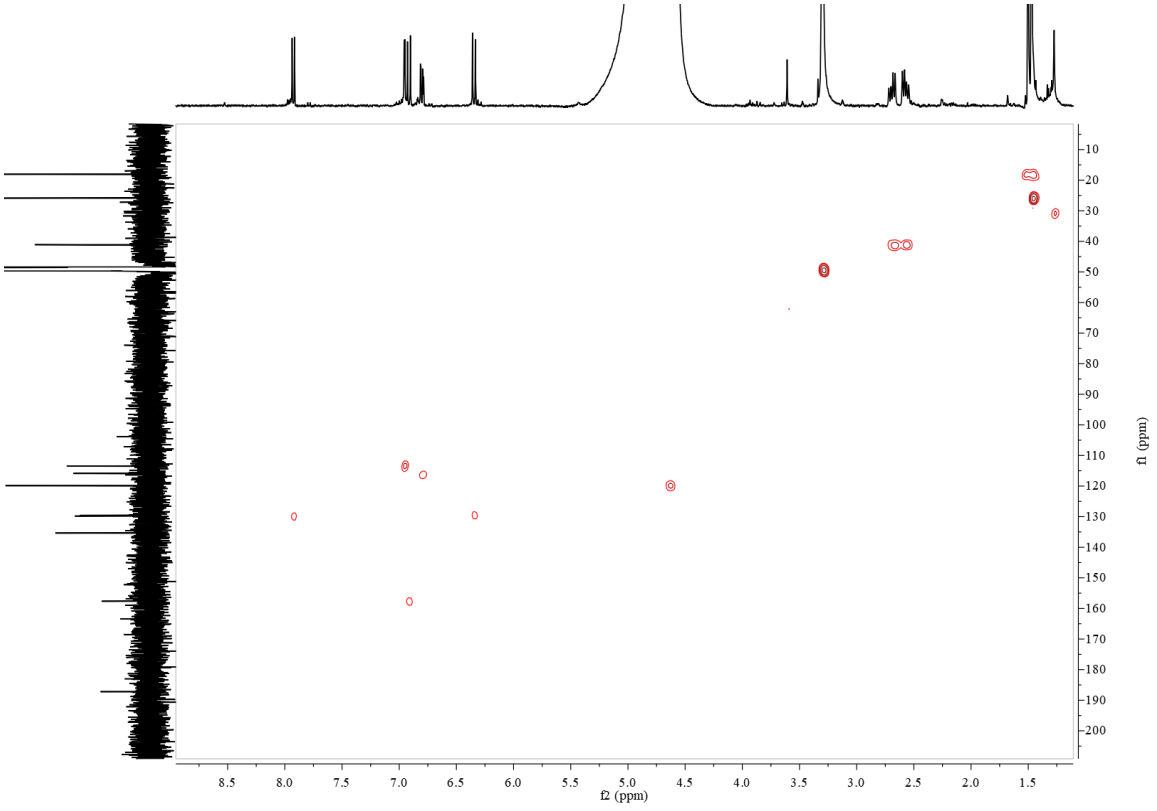

Figure S33: HSQC spectrum of **3D2** in CD_3OD (125 MHz).

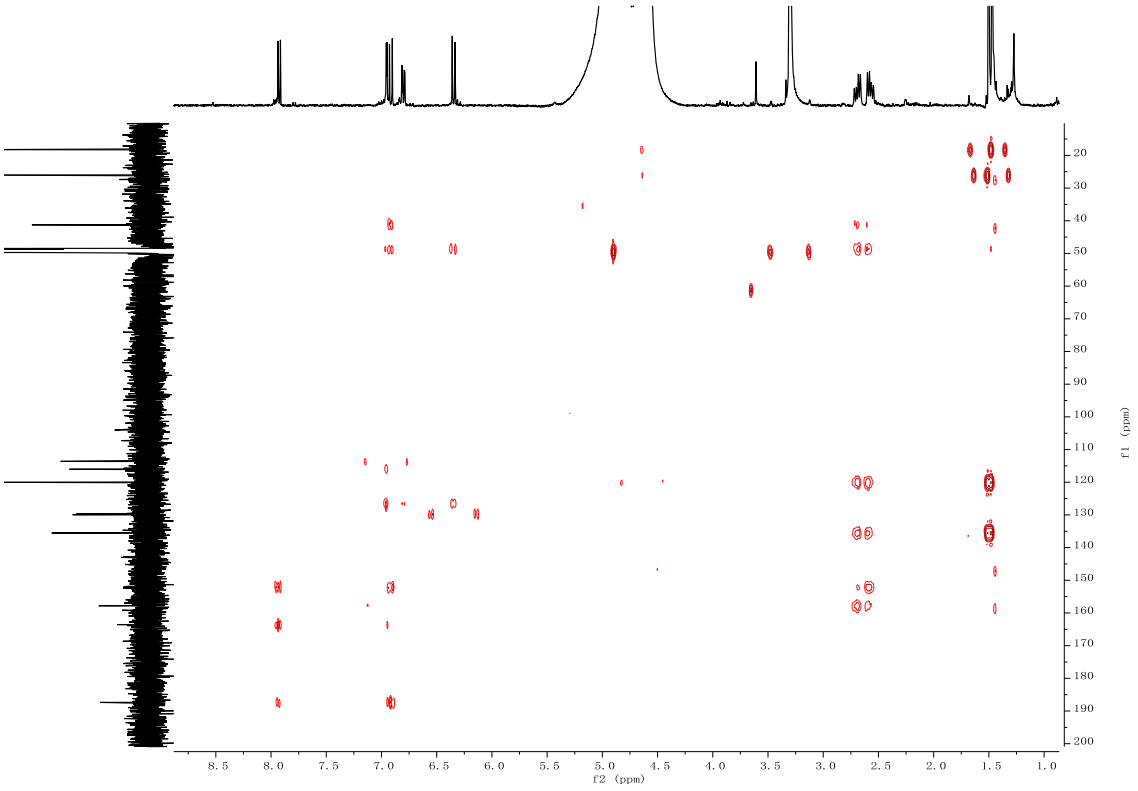

Figure S34: HMBC spectrum of **3D2** in CD_3OD (125 MHz).

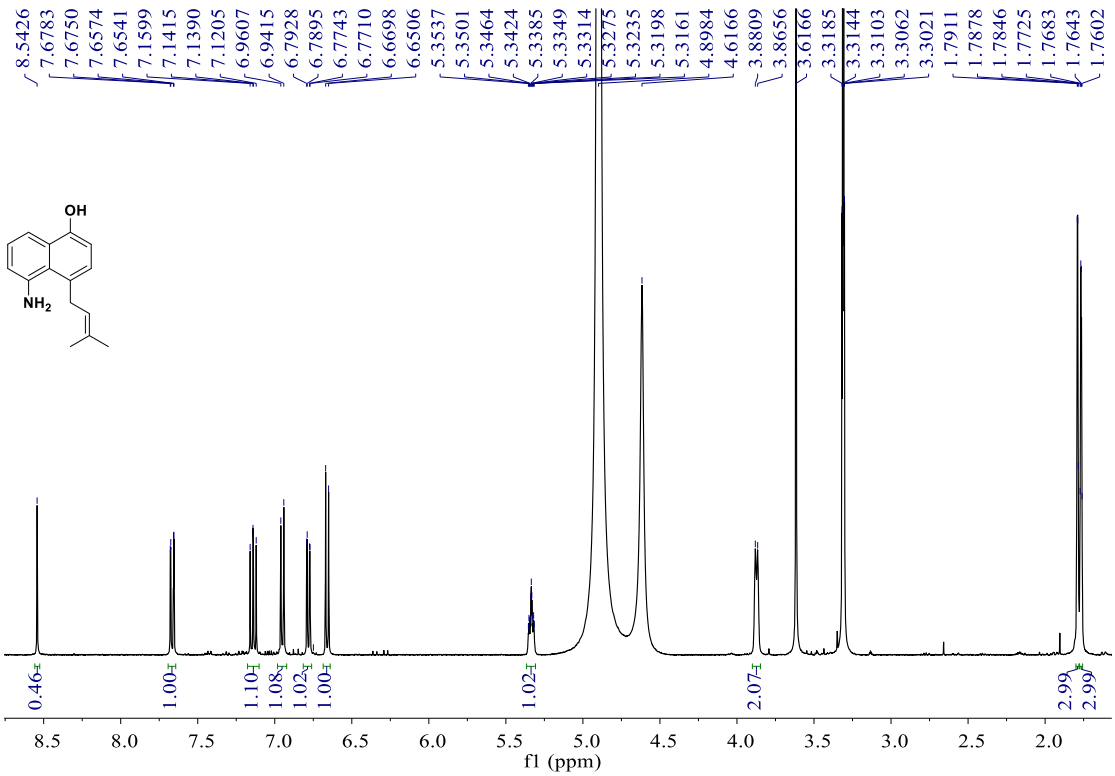

Figure S35: ^{1}H-NMR spectrum of **4D1** in CD_3OD (400 MHz).

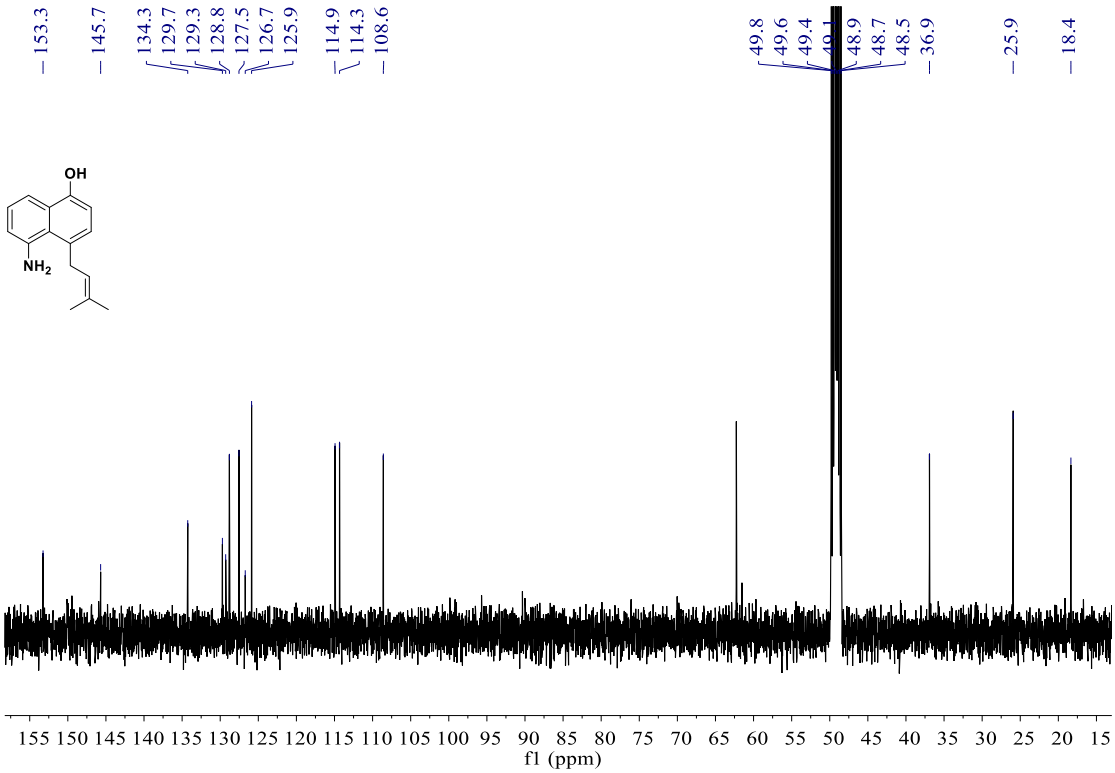

Figure S36: ^{13}C-NMR spectrum of **4D1** in CD_3OD (100 MHz).

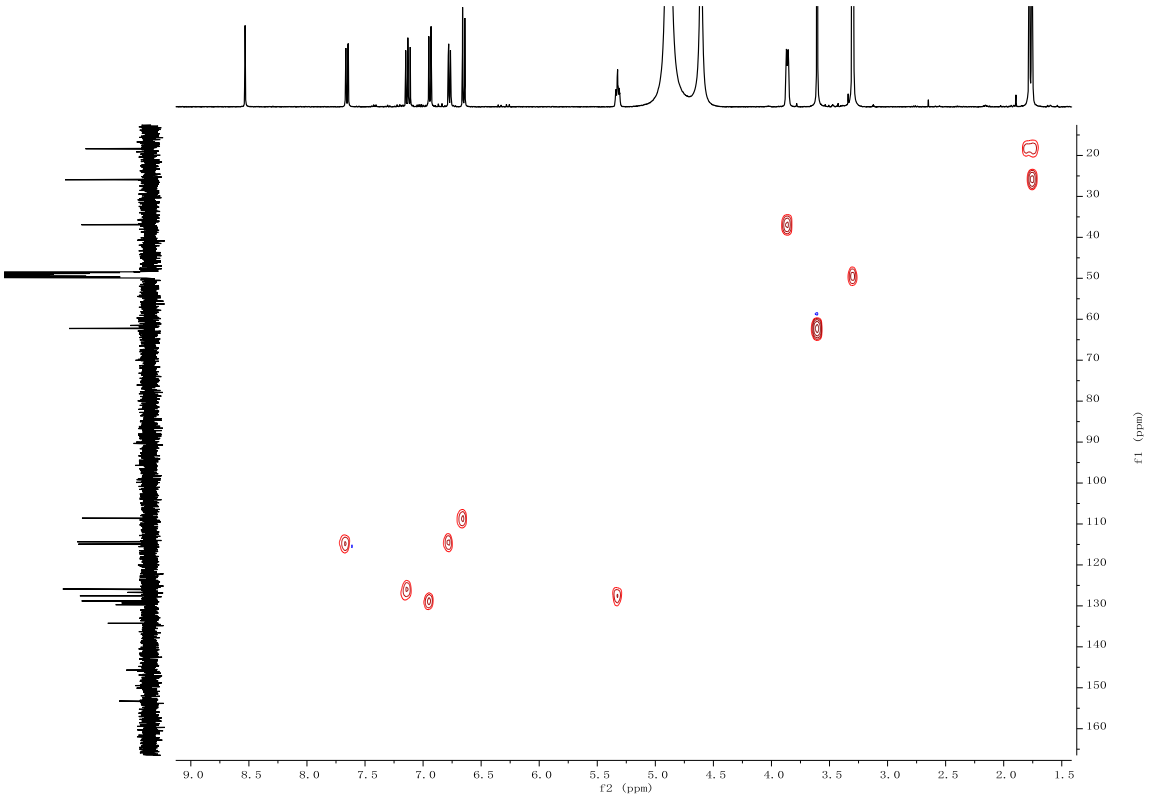

Figure S37: HSQC spectrum of **4D1** in CD_3OD (100 MHz).

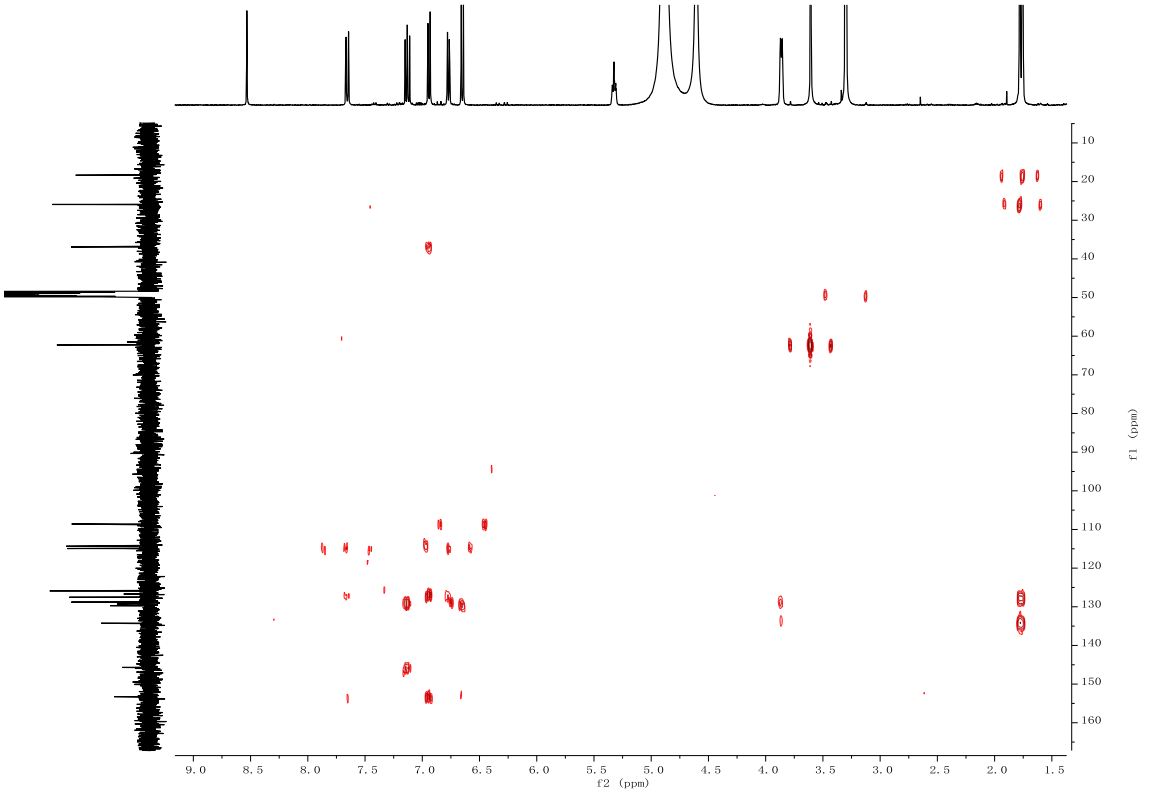

Figure S38: HMBC spectrum of **4D1** in CD_3OD (100 MHz).

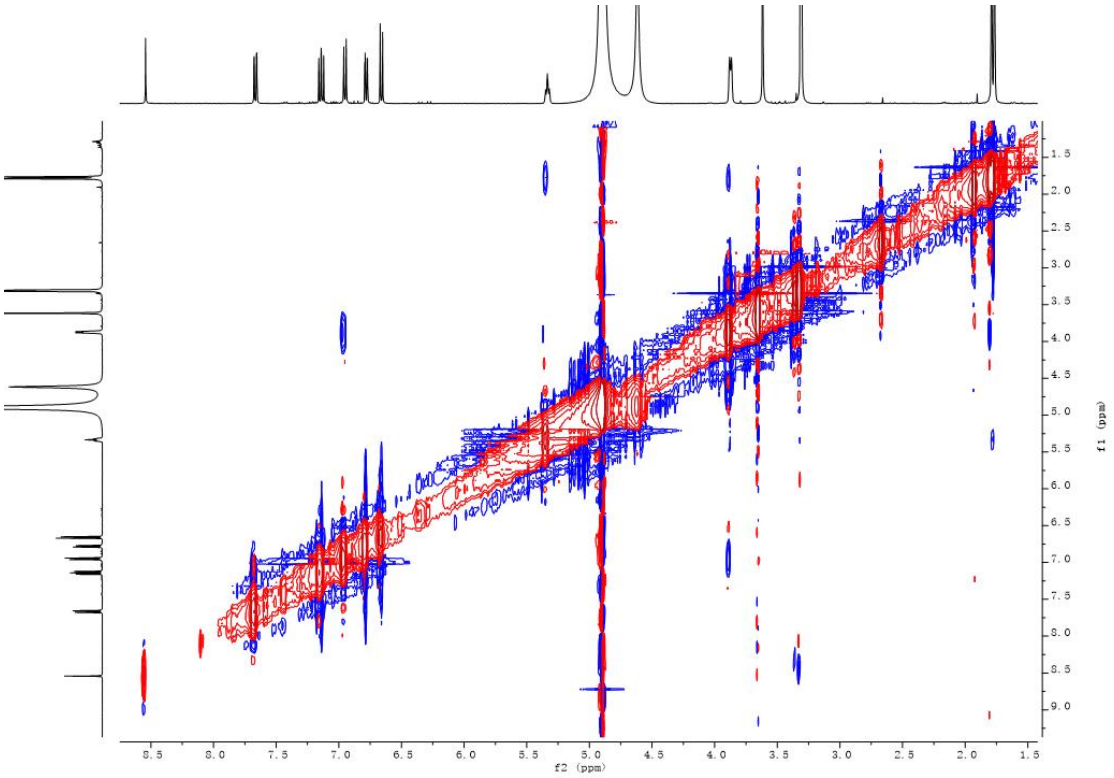

Figure S39: NOESY spectrum of **4D1** in CD_3OD (400 MHz).

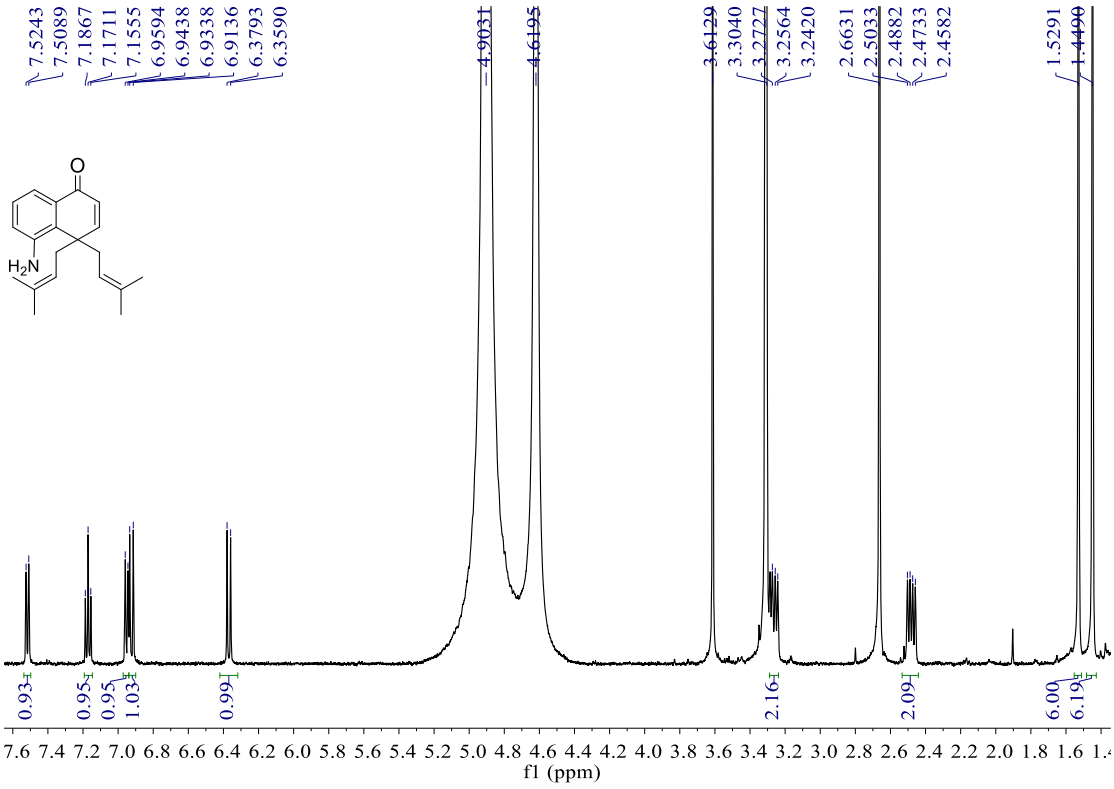

Figure S40: ^{1}H-NMR spectrum of **4D2** in CD_3OD (500 MHz).

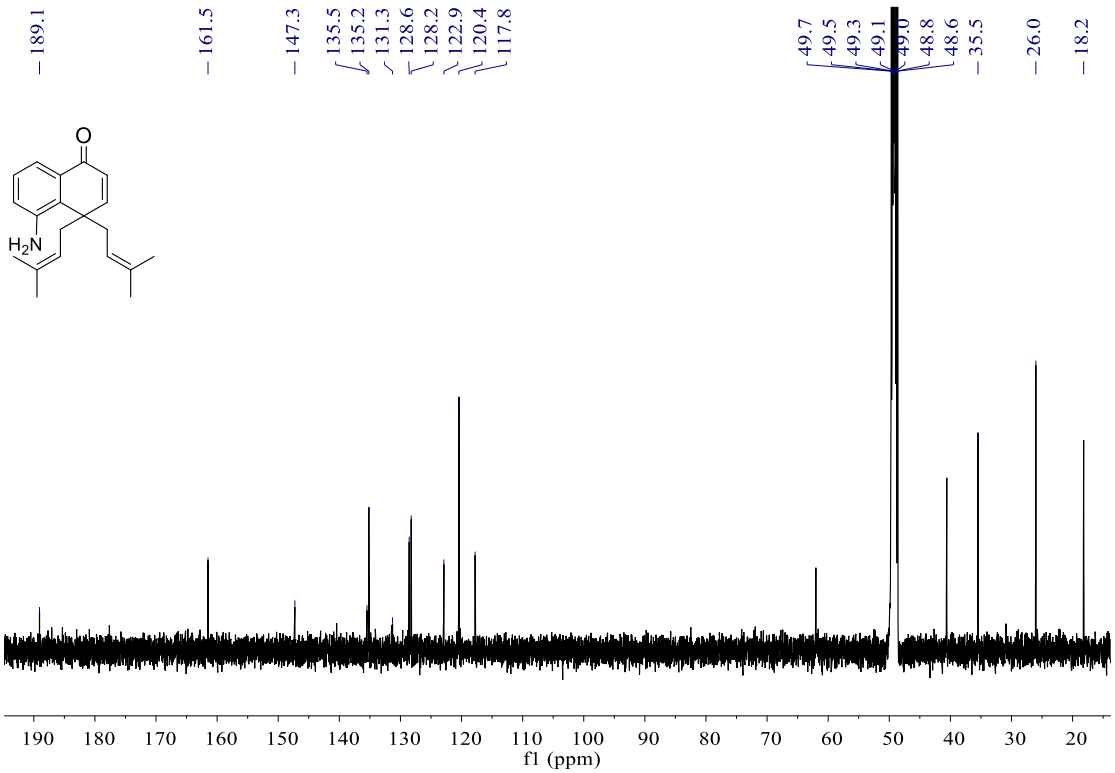

Figure S41: ^{13}C-NMR spectrum of **4D2** in CD_3OD (125 MHz).

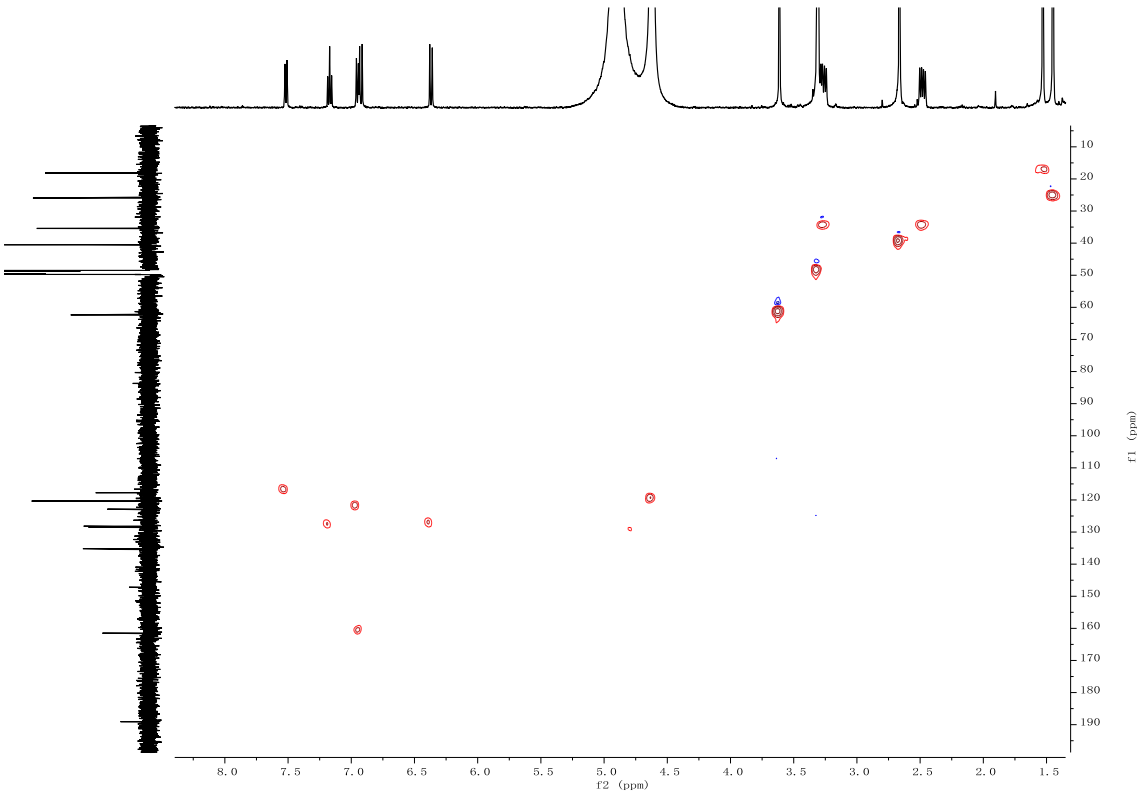

Figure S42: HSQC spectrum of **4D2** in CD_3OD (125 MHz).

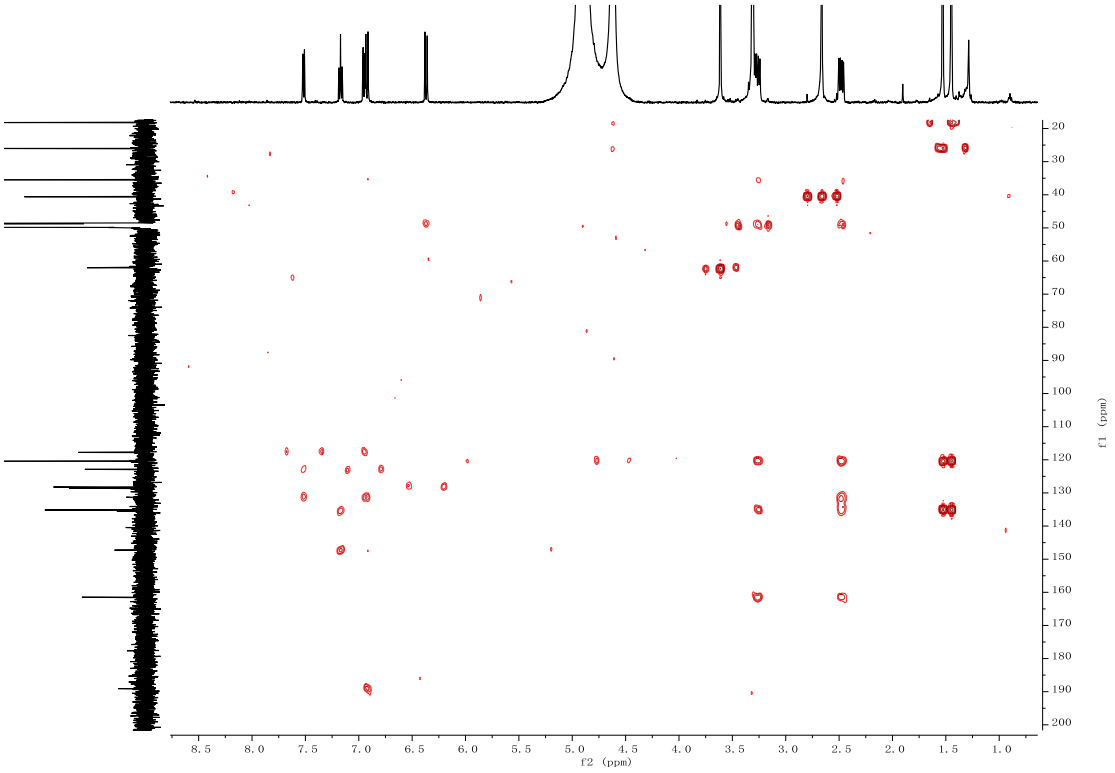

Figure S43: HMBC spectrum of **4D2** in CD_3OD (125 MHz).

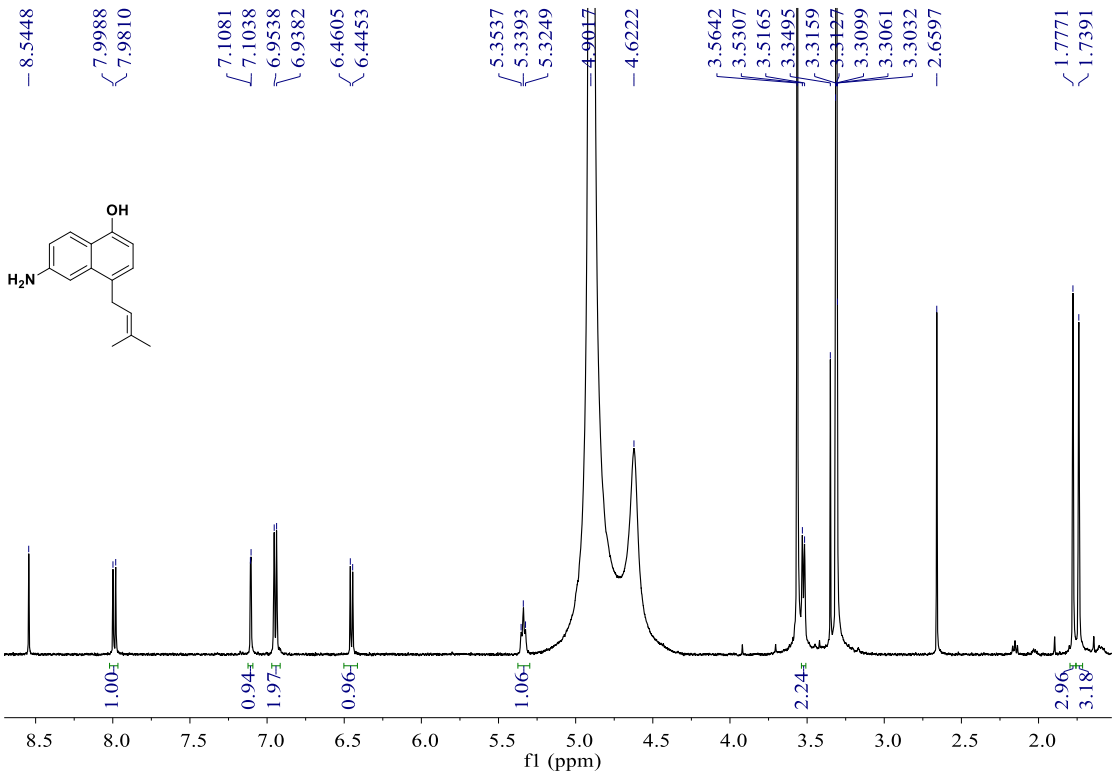

Figure S44: ^{1}H-NMR spectrum of **5D1** in CD_3OD (500 MHz).

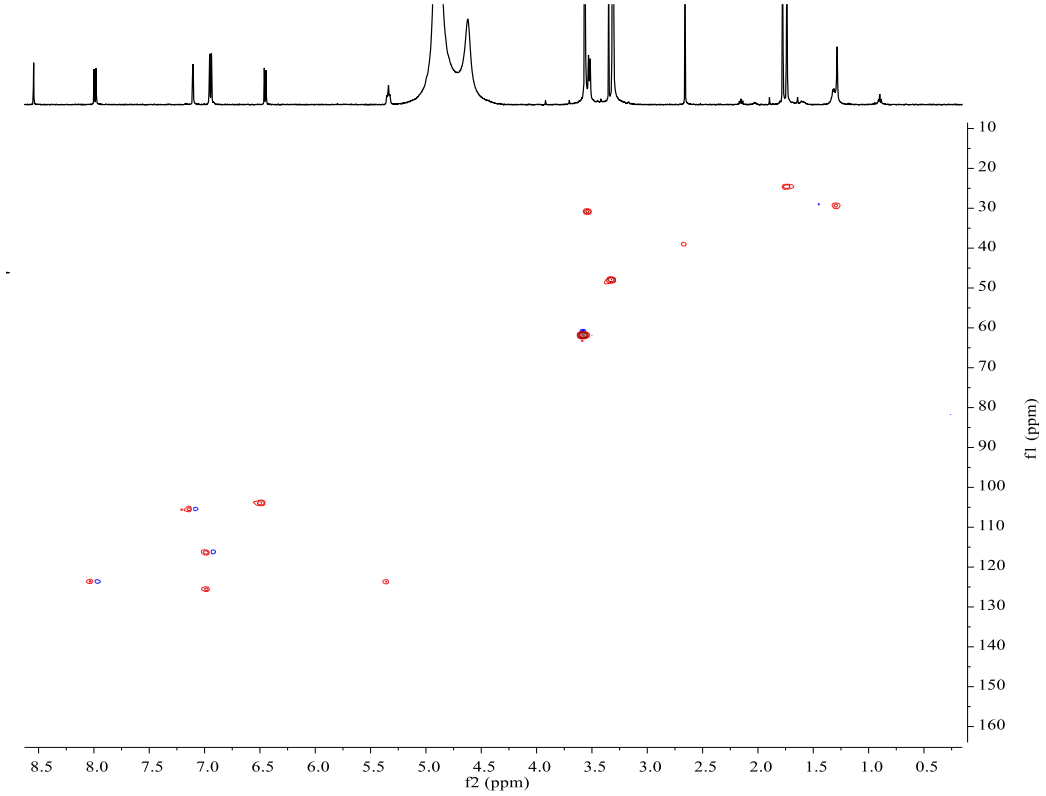

Figure S45: HSQC spectrum of **5D1** in CD_3OD (125 MHz).

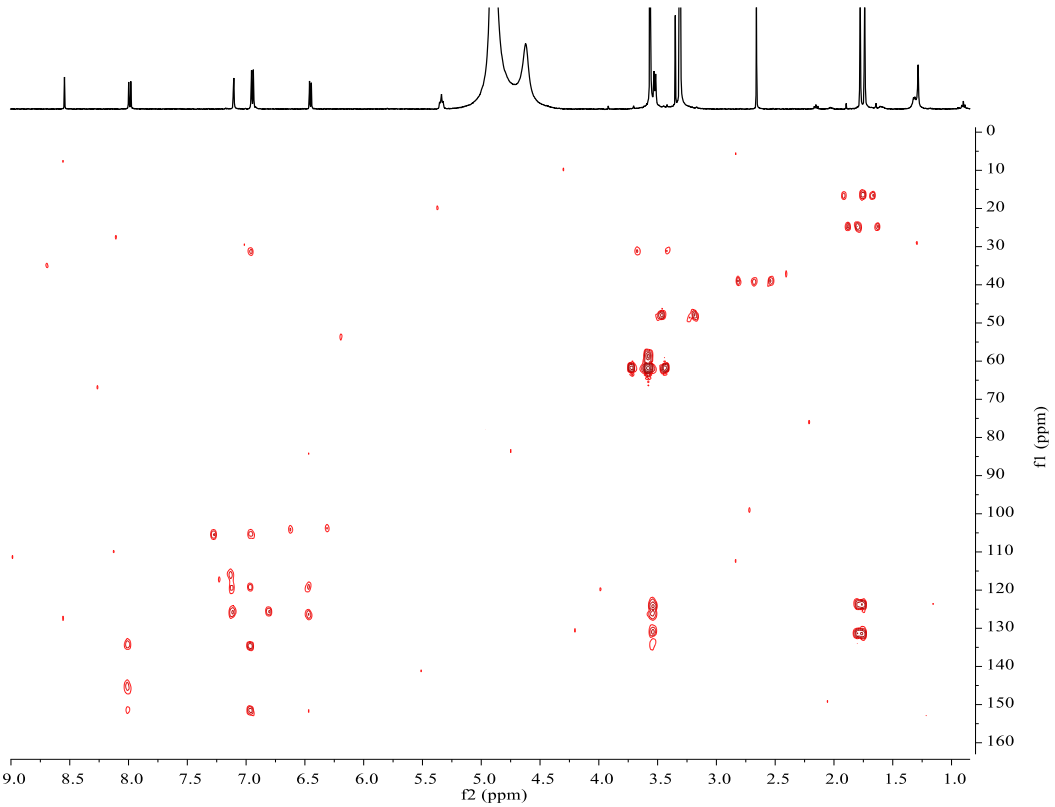

Figure S46: HMBC spectrum of **5D1** in CD_3OD (125 MHz).

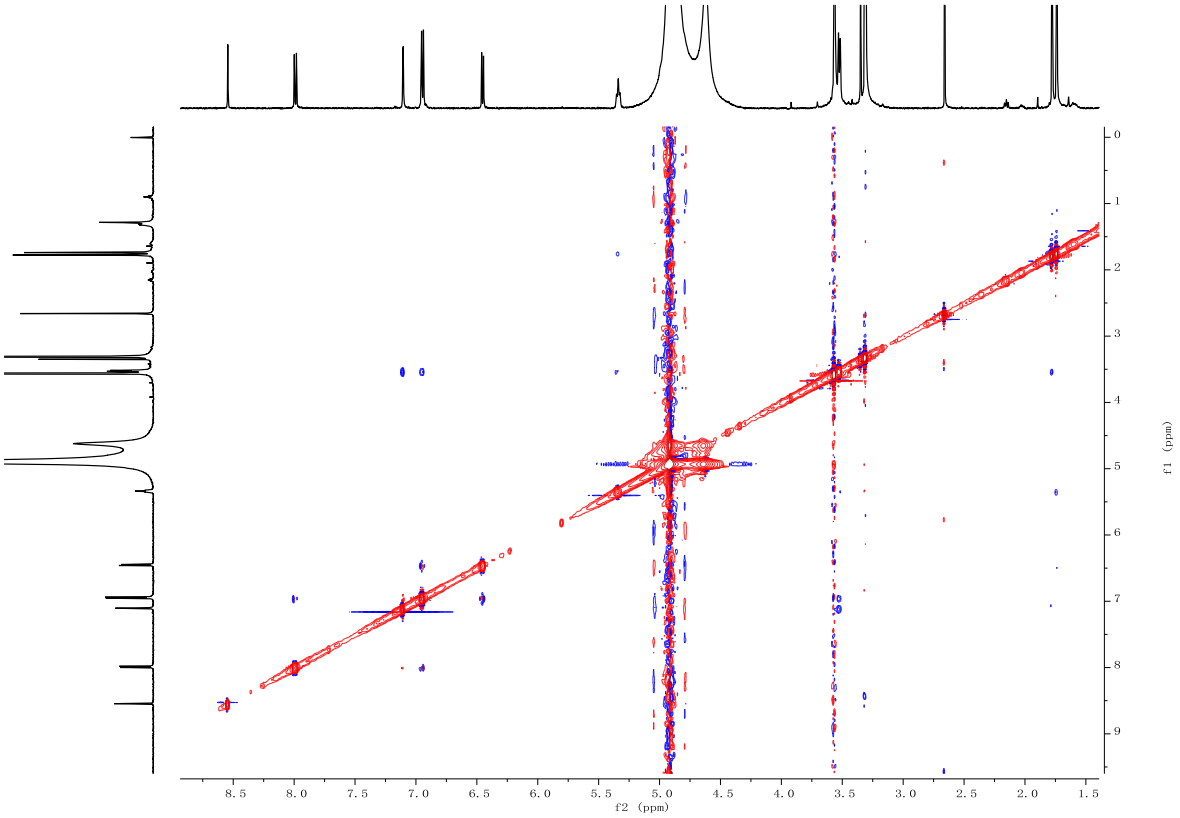

Figure S47: NOESY spectrum of **5D1** in CD_3OD (500 MHz).

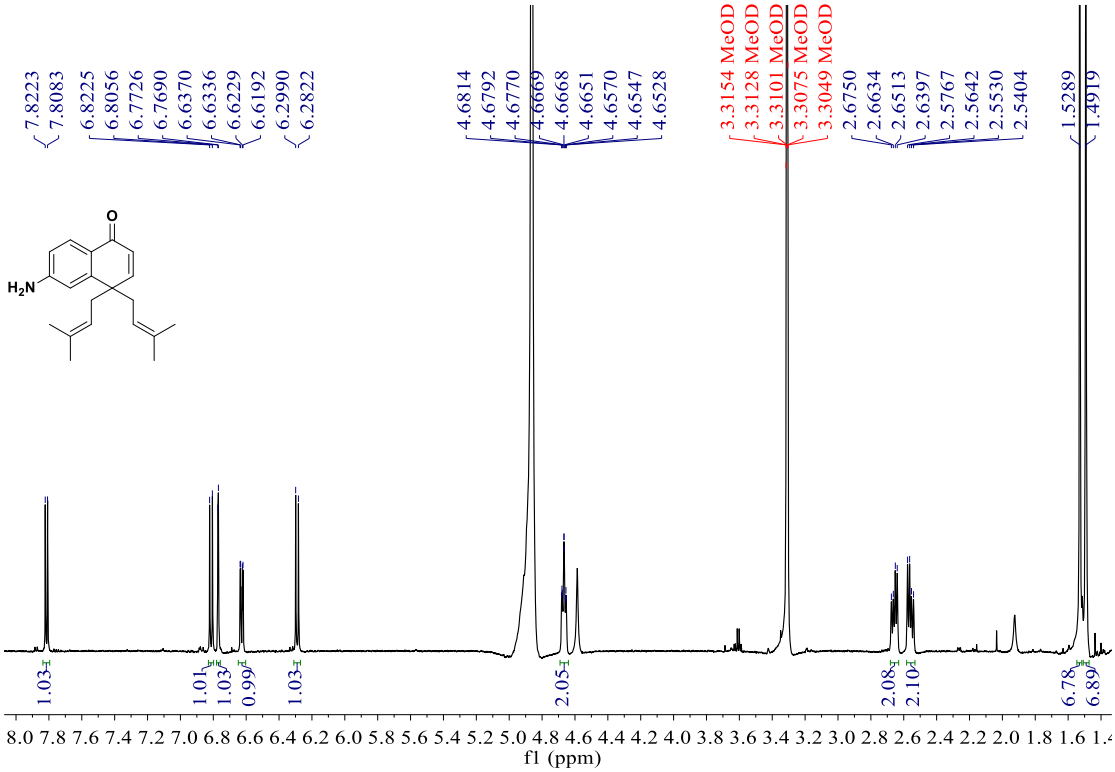

Figure S48: ^{1}H-NMR spectrum of **5D2** in CD_3OD (500 MHz).

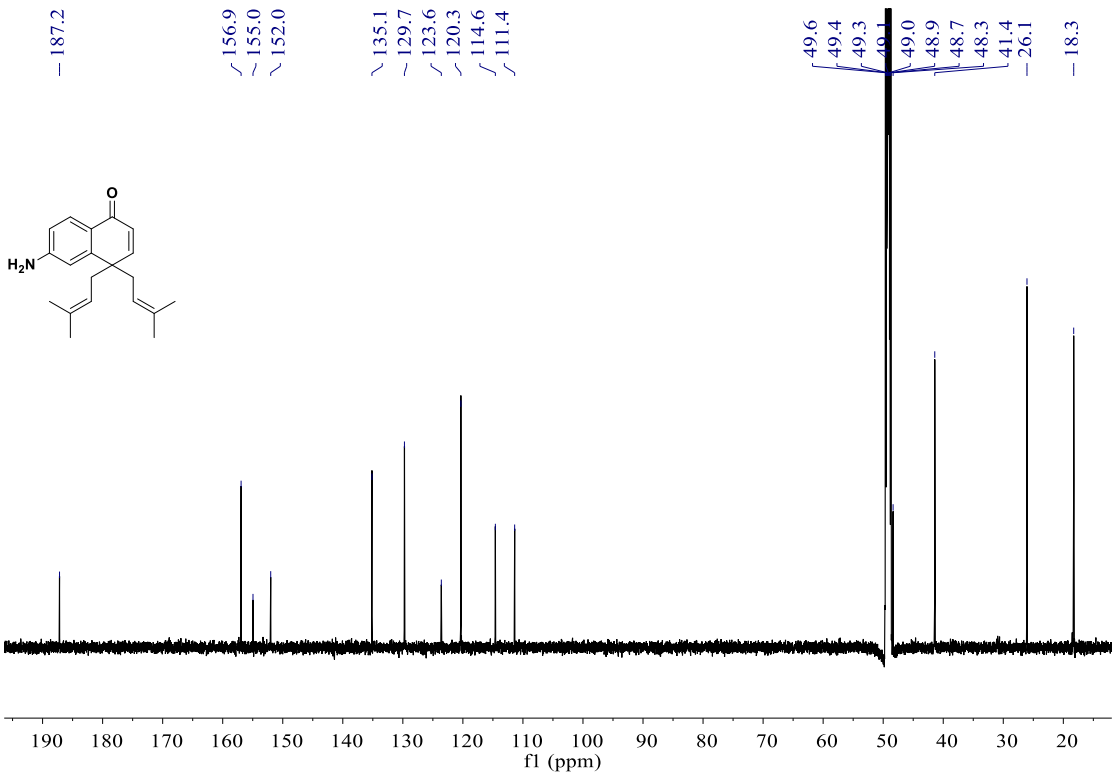

Figure S49: ^{13}C-NMR spectrum of **5D2** in CD_3OD (125 MHz).

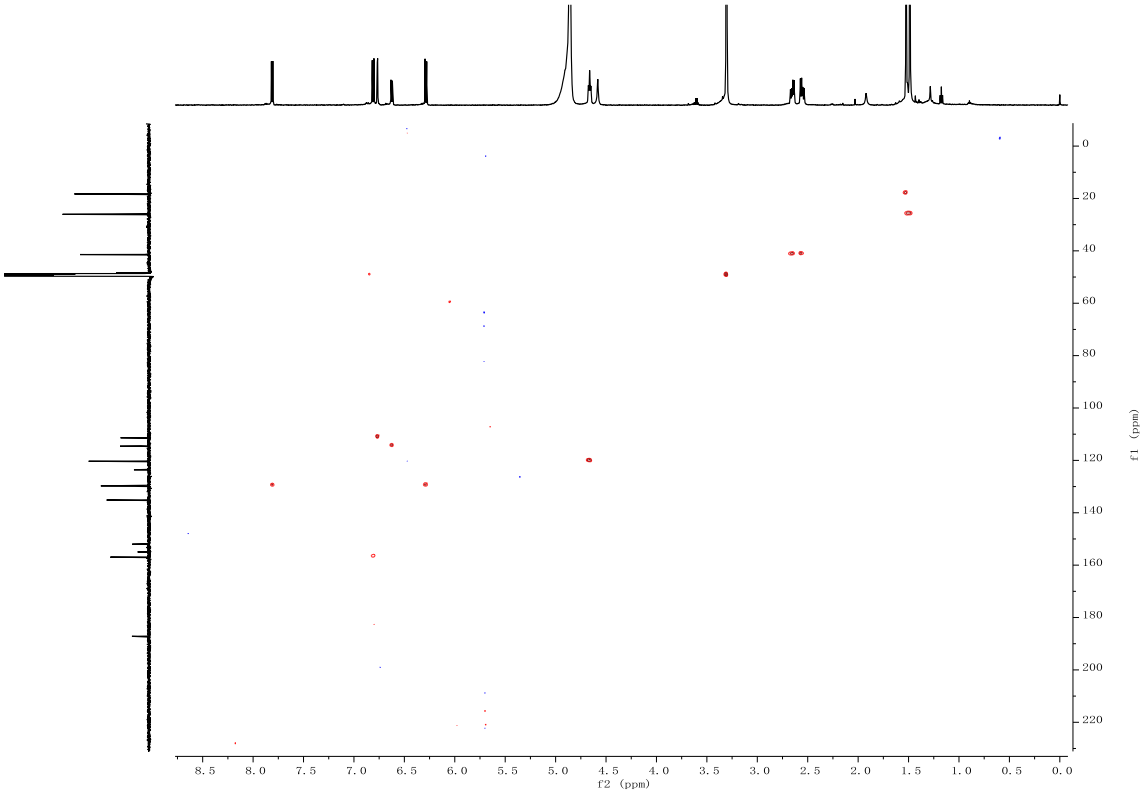

Figure S50: HSQC spectrum of **5D2** in CD_3OD (125 MHz).

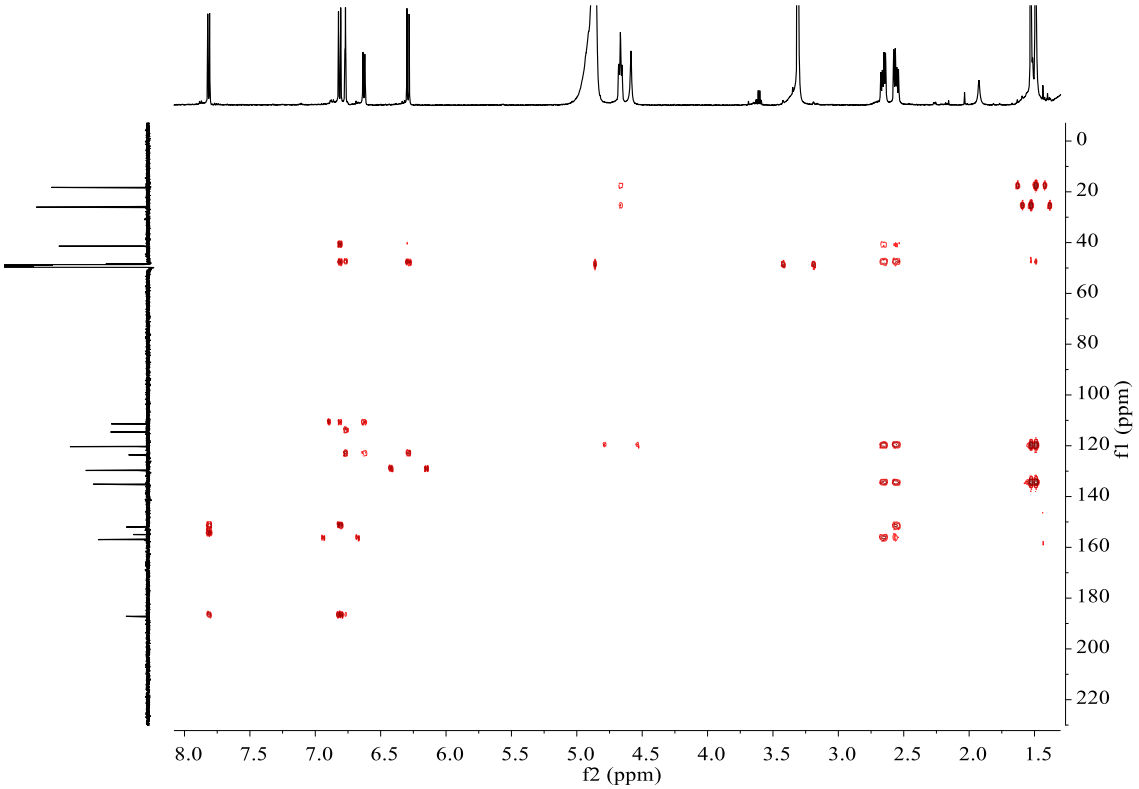

Figure S51: HMBC spectrum of **5D2** in CD_3OD (125 MHz).

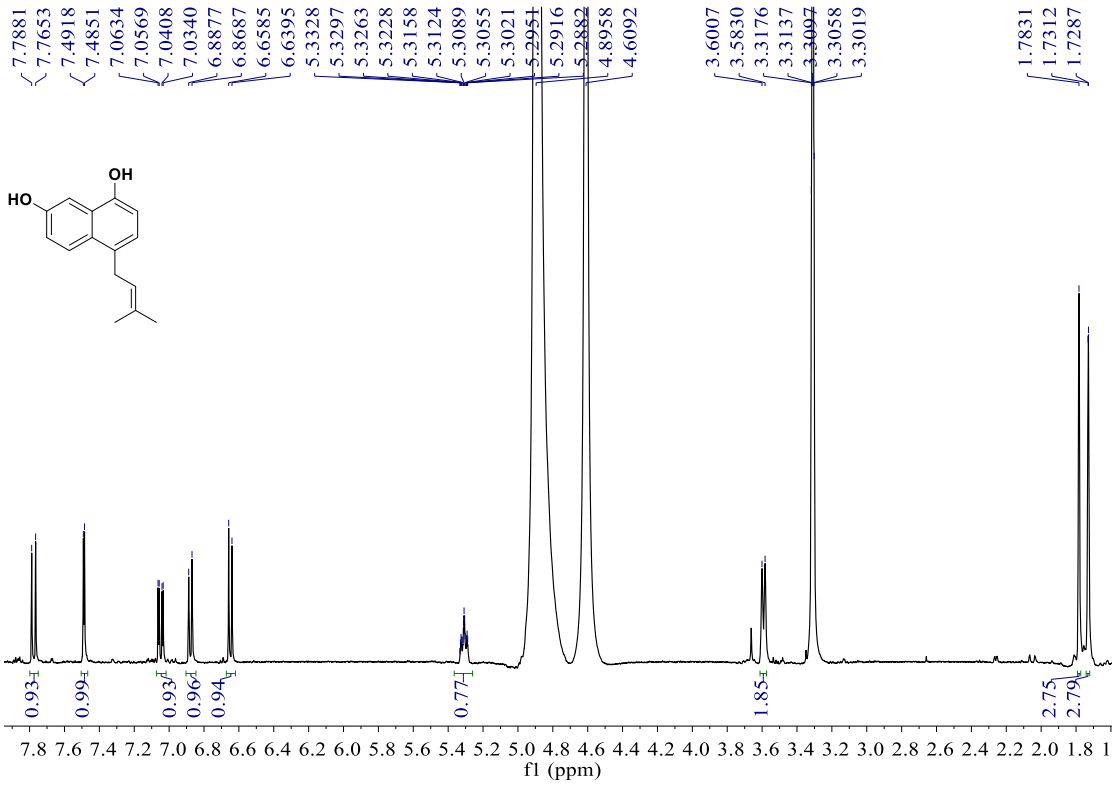

Figure S52: ^{1}H-NMR spectrum of **6D1** in CD_3OD (400 MHz).

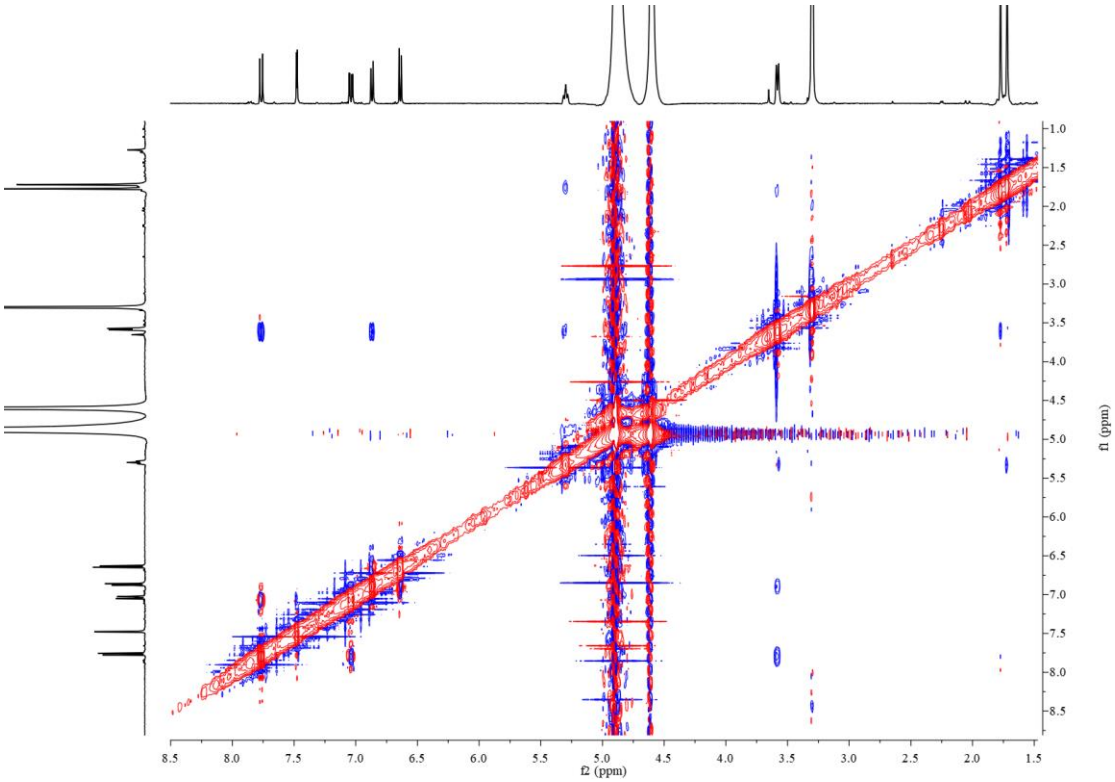

Figure S53: NOESY spectrum of **6D1** in CD_3OD (400 MHz).